N 73-27325

NASA SP-8021

NASA
SPACE VEHICLE
DESIGN CRITERIA
(ENVIRONMENT)

MODELS OF EARTH'S ATMOSPHERE (90 TO 2500 KM)

REVISED
MARCH 1973

NATIONAL AERONAUTICS AND SPACE ADMINISTRATION

FOREWORD

NASA experience has indicated a need for uniform criteria for the design of space vehicles. Accordingly, criteria have been developed in the following areas of technology:

Environment

Structure

Guidance and Control

Chemical Propulsion

Individual components of this work are issued as separate monographs as soon as they are completed. A list of the monographs published in this series can be found on the last page.

These monographs are to be regarded as guides to design and not as NASA requirements, except as may be specified in formal project specifications. It is expected, however, that the monographs will be used to develop requirements for specific projects and be cited as the applicable documents in mission studies, or in contracts for the design and development of space vehicle systems.

This monograph replaces a monograph of May 1969 on the Earth's upper atmosphere which provided a model for predicting atmospheric parameters at altitudes between 120 and 1000 km. The current model given herein covers a wider range – 90 to 2500 km – and provides improved predictions of atmospheric parameters.

This monograph was prepared under the cognizance of the Goddard Space Flight Center with Scott A. Mills of Goddard Space Flight Center and Robert E. Smith of Marshall Space Flight Center as program coordinators. The principal author was George Y. Lou of Northrop Services, Inc. The author is indebted to his colleagues, Richard L. King and Wallace W. Youngblood, for their valuable suggestions and criticism in the preparation of this monograph.

Comments concerning the technical content of these monographs will be welcomed by the National Aeronautics and Space Administration, Goddard Space Flight Center, System Reliability Directorate, Greenbelt, Maryland 20771.

March 1973

CONTENTS

MODELS OF EARTH'S ATMOSPHERE (90 to 2500 km)

1. INTRODUCTION

Atmospheric conditions encountered by a spacecraft in orbit about the Earth are important factors in space vehicle design, mission planning, and mission operations. Density is the primary atmospheric property that affects the spacecraft's orbital altitude, lifetime, and motion. Density directly affects the torques which result from aerodynamic interaction between the space vehicle and the atmosphere; such torques must be considered in design of spacecraft attitude control systems. Density scale height is required in heating calculations for space vehicles re-entering the Earth's upper atmosphere. Density as well as chemical composition and temperature are needed in calculating a spacecraft's drag coefficient. Chemical composition and temperature also are required in the design of some experiment sensors to be flown in the upper atmosphere.

Because of variability of atmospheric conditions with spatial location and solar activity, invariant models of the Earth's atmosphere (90 to 2500 km) would not be useful for most engineering applications. Therefore this monograph presents a computerized version of a model atmosphere developed by Jacchia in 1970 (ref. 1) that incorporates variation with solar activity and spatial location. The computerized model can provide at selected times and locations estimates of density, composition, temperature, molecular mass, pressure scale height, and density scale height for altitudes between 90 and 2500 km.

This monograph replaces a monograph on the upper atmosphere which was a computerized version of Jacchia's 1964 model (ref. 2). The current model has a range from 90 to 2500 km; the model in the earlier monograph extended from 120 to 1000 km. The assumed boundary conditions at 120 km in the earlier monograph led to misrepresentation of atmospheric conditions below 200 km. Additional data from rocket probes and low-altitude satellites made possible the development of the improved model recommended herein.

In addition to the computerized technique, this monograph gives a quick-look prediction method that may be used to estimate the density for any time and spatial location without using a computer. Sample problems illustrate this method.

Information in this monograph applies to altitudes between 90 and 2500 km; another monograph (NASA SP-8084) gives extreme atmospheric conditions at launch sites and another monograph is to give in-flight atmospheric extremes from the launch sites to an altitude of 90 km. Other design criteria monographs on the Moon, other planets, and space vehicle technology are listed at the end of this monograph.

2. STATE OF THE ART

Model atmospheres of the upper atmosphere have been developed that use assumed physical relationships in conjunction with observed phenomena (refs. 3 and 4). However, incomplete knowledge of the physics of the upper atmosphere limits the value of the resulting models for engineering purposes.

This monograph concerns itself with model atmospheres that have empirical coefficients (derived mainly from analysis of changes in periods of orbiting satellites) which relate neutral densities to solar flux, geomagnetic activity, time of day, latitude, and season.

Since the publication of reference 5, a more detailed picture of the structure of the Earth's upper atmosphere has emerged from additional satellite and rocket measurements, particularly in the altitude region below 200 km. As a result, the representativeness of the atmospheric models has been greatly improved. For example, the models recently published in references 1 and 6 have removed the long-recognized drawback of the invariance of the boundary conditions at 120 km; consequently, the atmospheric variability at that altitude and the altitude region immediately above it are represented better. In addition, significant improvements have been made by increasing the O/O_2 ratio at 120 km and representing the semiannual effect as a change in density rather than in exospheric temperature. From the space vehicle design and planning standpoint, the models of the Earth's upper atmosphere given in references 1 and 6 appear to be the best available to date. Because the model given in reference 1 has been proven to yield better results in orbital lifetime predictions than its later version given in reference 6, the prediction method given in reference 1 was adopted in the present monograph.

An empirical model recently has become available that gives more detailed information on densities of individual gas species on the basis of OGO-6 data (ref. 7).

2.1 Earth's Upper Atmosphere

2.1.1 Terms of Reference

For purposes of reference, the Earth's atmosphere is often divided into regions. In the most commonly used system, these regions are differentiated by thermal stratification. The lowest region, extending from ground level to the first temperature minimum, is called the troposphere. The next region, which extends up to the level with maximum temperature, is called the stratosphere. The third region, which extends up to the second temperature minimum, is the mesosphere. The region directly above the mesosphere is the thermosphere. Beyond the thermosphere is another region called the exosphere, but the latter is not defined by its temperature distribution. These terms and other terms that identify regions characterized by other phenomena are given in the Glossary (appendix C).

Besides the foregoing divisions, the atmosphere often is divided into a lower and an upper region with the choice of altitude to separate them being somewhat arbitrary. In the present monograph, the term "upper atmosphere" is adopted to designate the portion of the atmosphere above 90 km in altitude.

2.1.2 Variation of Composition and Temperature with Altitude

A brief description of the phenomena associated with the variations in composition and temperature with altitude is helpful for an understanding of the upper atmosphere. In the homosphere, the mixture of gasses is distributed vertically in quasi-hydrostatic equilibrium, with turbulent mixing keeping the relative composition of the atmosphere constant from the Earth's surface to an altitude of about 90 km. Thus a given temperature profile in the homosphere can uniquely determine the corresponding density distribution to be associated with a pressure value at a given lower altitude.

As the altitude increases, photodissociation processes cause the composition to change, resulting in a decrease of the molecular mass with height, primarily from replacement of molecular oxygen by atomic oxygen. At higher altitudes, diffusive separation becomes dominant so that each individual gas is distributed by altitude according to its own molecular mass. Consequently, the abundance of lighter gasses, such as atomic oxygen, atomic nitrogen, atomic hydrogen, and helium, decreases less rapidly with height than is the case for the heavier gasses. Above certain altitude levels these lighter gasses predominate over the heavier ones. It is then difficult to determine the distribution of mean molecular mass. Thus, a given temperature profile will not define a unique density profile in the heterosphere.

Because of the long and short term variations in the upper atmosphere, there is no unique altitude that defines the base of the heterosphere. It occurs somewhere between 80 and 100 km above the Earth and closely coincides with the base of the thermosphere. The thermosphere extends to an average altitude of about 500 km. The upper limit of the thermosphere, i.e., the thermopause, varies with the level of solar activity. During periods of minimum solar activity, the thermopause occurs at about 350 km; during periods of maximum solar activity, it can be as high as 700 km. Above the thermopause is the region known as the exosphere. In this region, atoms of hydrogen and helium can break loose from the Earth's gravitational field because of their lightness and energy and escape into outer space. In the lower exosphere, the most abundant atom is oxygen. At higher altitudes, the most abundant atom is helium, and at still higher altitudes, atomic hydrogen.

A basic feature of the structure of the thermosphere is the very steep increase in temperature with height from 90 to 200 km. This is because of absorption of solar radiation primarily with wavelengths up to 2000 Å, particularly in the extreme ultraviolet (EUV) portion of the spectrum (ref. 8). The absorbed radiation causes dissociation and ionization of particles, and consequent release of heat. For altitudes above approximately 200 km, the heat deposited in the atmosphere decreases with altitude and the atmosphere approaches isothermality if there is not appreciable heat input from magnetosphere.

2.2 Variations in Atmospheric Parameters With Location and Solar Condition

The vast number of determinations of the drag exerted by the atmosphere on satellites and measurements made by density gauges and mass spectrometers aboard rockets and satellites have revealed seven different effects other than altitude that result in variations of density, temperature, and composition of the upper atmosphere. These observed variations are:

- Variations with solar activity
- Diurnal variation
- Variations with geomagnetic activity
- Semiannual variation
- Seasonal-latitudinal variations of the lower thermosphere
- Seasonal-latitudinal variations of helium
- Rapid density fluctuations probably associated with tidal and gravity waves

Each of these variations have been taken into account in the model adopted herein except for the variations associated with tidal and gravity waves. More information can be found in references 1, 6, and 9.

2.2.1 Variation with the Solar Activity

The solar ultraviolet radiation impinges upon the Earth's upper atmosphere continuously, but with variable spectral intensity distribution according to solar conditions. It is the UV and EUV radiation that heats and causes structural changes in the upper atmosphere. There are two components of this radiation that generate heat energy. The one that relates to active regions on the solar disk varies from day-to-day, whereas the one that relates to the solar disk itself varies more slowly with the 11-year solar cycle. The atmosphere has been observed to react to each of these two components in a different manner (ref. 1). Separate values of the two components of the solar flux are not readily available; however, the observations made by OSO 1 in 1962 have confirmed that the integrated EUV flux and the 10.7-cm radiation (a quantity readily measurable at the Earth's surface) are proportional to each other.

In the thermosphere, the density is strongly influenced by the changing levels of solar activity. The resulting density variations, in turn, affect the frictional air drag on satellites. The relationship between solar activity and the air drag exerted on satellites was first recognized by Jacchia in 1958 (ref. 10). From the study of the orbits of Sputnik III and Vanguard 1, he found that the air drag increased considerably in periods of high solar activity. During these periods of solar flares and other solar disturbances, the Sun's ultraviolet and corpuscular radiation increase markedly; the result is greater heating of the Earth's upper atmosphere. Subsequent studies of satellite drag data have verified a pronounced correlation between solar activity and density variations (refs. 11 through 14). However, the reaction of the atmosphere to variations of the Sun is not instantaneous. From analysis of the time lag between EUV flux from OSO-1 and exospheric temperatures computed by Jacchia and Slowey (ref. 15), Bourdeau et al. (ref. 16) concluded that the atmospheric response time was on the order of one day. Recently, Roemer (refs. 17 and 18) found a time lag of 1.0 ±0.12 days in the 355 to 710 km altitude range on the basis of data from six satellites.

2.2.2 The Diurnal Variation

2.2.2.1 Density

The diurnal variation of density in the Earth's upper atmosphere has been observed by satellite drag measurements. From approximate equality between day and night densities at 200 km, the excess density of day over night increases with altitude; at 600 km the daytime density can be higher by a factor of eight (ref. 19). This day-to-night ratio has also been observed to be strongly latitudinal dependent; the larger values are found at lower latitudes and smaller values at higher latitudes (ref. 20). Results of satellite drag measurements have clearly shown that the density has a maximum around 1400 local solar time at a latitude approximately equal to that of the subsolar point, and a minimum around 0300 hours at about the same latitude in the opposite hemisphere. The effect is believed to be caused by the absorption of EUV radiation and by heat conduction of the neutral gas. The energy that is conducted downward into the lower thermosphere and mesosphere is mostly lost by radiation processes. At an altitude of about 120 km, the time constant for heat loss by conduction is on the order of one day or greater (ref. 19). Thus, the diurnal variation is not a predominant phenomenon at lower altitudes.

Theoretically, a satisfactory explanation of the diurnal process can be obtained by solving the hydrodynamic and thermodynamic equations; however, attempts made by Harris and Priester (ref. 21) and later by Mahoney (ref. 22) gave results that are not in agreement with the observed phenomena; e.g., the calculated diurnal bulge occurs about 1700 local solar time compared with the observed occurrence at about 1400. This discrepancy has been explained to be the result of not taking into account the horizontal energy transport. Subsequent studies especially those by Volland, Stubbe, and Mayr (refs. 3 and 23 through 26), on the effect of horizontal wind on the shape of the diurnal temperature and density distribution did indicate a reduction of the time lag between theoretical and observed bulges, but the problem has not been totally resolved.

Also, related studies have been made on derivation of thermospheric winds from pressure gradients of the diurnal bulges (refs. 27 through 33). Harris (ref. 29) has shown that the effect of ion drag on neutral particles has an important bearing on wind velocities. Use by Harris (ref. 29) of the electron density profile of Chandra (ref. 34) and the collision frequency between neutral and ions of Chapman (ref. 35) led to a shift of the calculated bulge one hour earlier to 1600 local solar time.

2.2.2.2 Temperature

The diurnal variation of temperature in the thermosphere has been obtained from analyses of observations of satellite drag and the ground-based incoherent scatter technique. There is a large discrepancy in the phase of the variations as inferred from these two types of observations. Chandra and Stubbe (ref. 36) concluded from a case study that this discrepancy can be fully reconciled by introducing temperature and density perturbations at the base of the thermosphere; however, their analysis was later re-examined by Cummack and Butler (ref. 37) who concluded that the reaction of the thermosphere to temperature variations at the base of the thermosphere is small. The discrepancy has not been reconciled.

The amplitude of the diurnal temperature variation in the thermosphere is not constant. Through analyses of satellite drag data, Jacchia and Slowey (ref. 38) have shown that the maximum-to-minimum ratio of exospheric temperatures was about 1.32 from 1958 to 1963, then it dropped to 1.26 in the middle of 1963. This low value was maintained until 1967. The ratio of day-to-night exospheric temperature was also found not to depend completely upon solar activity although it tends to be higher during maximum solar activity and lower during minimum solar activity. A recent study (ref. 1) has concluded that this ratio has a fairly good correlation with the yearly running mean of the geomagnetic activity index K_p, but is independent of latitude. The numerical value of the ratio varies between 1.27 and 1.40 and has an average value of 1.31.

2.2.3 Variations with Geomagnetic Activity

2.2.3.1 Origin

Geomagnetic storms usually occur when clouds of charged particles collide with the Earth's magnetosphere. These charged particles are believed to be ejected from the Sun during the course of a solar flare which is generally a short-lived phenomenon. As a result, a large amount of solar radiation is emitted by the flare region which subsequently heats the Earth's atmosphere. The heating mechanism is not well-understood, but there have been some investigations (refs. 39 through 41).

2.2.3.2 Time Lag

Satellite observations have shown a time lag between the onset of geomagnetic disturbances and the subseqeunt observed increases in density. Early studies of Explorer 9 satellite drag data (refs. 15 and 17) showed this time lag to be about 5 hours. A recent investigation of high-inclination satellite data (ref. 42), however, has indicated that the atmospheric perturbation lags about 5.8 hours at high latitudes and that the time lag tends to increase towards the equator to 7.2 hours. From an analysis of LOGACS* data (ref. 43), the atmospheric density is found to respond to geomagnetic storms almost immediately near the polar region and to respond more slowly with increasing distance from the polar region. An average time lag is presently taken as 6.7 hours (ref. 1). There is also evidence that even the

*Low-G Accelerometer Calibration System

smallest variation in the magnetic field of the Earth, such as those observed during magnetically quiet days, is also reflected in density and temperature variations in the upper atmosphere (refs. 44 and 45). There is recent evidence from the OGO-6 mass spectrometer that the atmospheric response to magnetic activity is dominated by N_2 increases at high latitudes (ref. 46), and this information may be reflected in a subsequent revision of this monograph.

2.2.4 The Semiannual Variation

Semiannual variation of the atmospheric density was first discovered by Paetzold and Zschorner (refs. 47 and 48) from satellite drag measurements in the altitude range of 210 to 650 km. It was later confirmed by Cook and Scott (ref. 49) at an altitude of 1130 km and by King-Hele and Hingston (ref. 50) at 190 km. The outstanding characteristics of the semiannual density variation are a primary minimum in July, followed by a high maximum in October, and a secondary minimum in January, followed by a secondary maximum in April. More recent analyses of satellite drag data (ref. 51) show that the semiannual variation in density in the 150 to 180 km altitude region is similar to that at higher altitudes. It has also been found (ref. 52) that the semiannual effect varies considerably from solar cycle to solar cycle, both in magnitude and in altitude dependence. According to Jacchia (ref. 2), the amplitude of this variation is quite large at sunspot maximum but decreases toward sunspot minimum.

The cause and mechanism of the semiannual variation are not yet fully understood. Early hypotheses are considered in references 48 and 53. References 54, 55, and 56 are recent attempts to explain this phenomenon.

2.2.5 Seasonal-Latitudinal Variations of the Lower Thermosphere

Recent low-altitude, high-inclination satellite and rocket probe measurements have shown that the lower thermosphere is subject to a large seasonal-latitudinal variation in temperature and a smaller variation in density. The amplitude of the density variation was found to increase very rapidly with height from 90 km up to a peak somewhere between 105 and 120 km (refs. 57 and 58) and then to decrease with altitude to 200 km where no appreciable seasonal-latitudinal variation has been observed (refs. 38 and 59). At higher altitudes, however, a density anomaly in the auroral region has been reported by Newton and Pelz (ref. 60), Philbrick and McIsaac (ref. 61), and Allan (ref. 62). A density bulge at altitudes below 200 km in the auroral region had been previously found by Jacobs (ref. 63) and Marcos et al. (ref. 64); this has been confirmed by recent analyses of the OVI 15 satellite drag data (ref. 65).

2.2.6 Seasonal-Latitudinal Variation of Helium

Reber and Nicolet (ref. 66) first noted the enhancement of helium toward the winter hemisphere in the analysis of mass spectrometer data from Explorer 17.

From the analyses of orbital decay of the Explorer satellites, Keating and Prior (ref. 67) observed a winter density bulge in the polar exosphere which they attributed to the peak helium concentration at high latitudes in the winter hemisphere (refs. 68 and 69). This finding has been confirmed by other independent satellite drag measurements (refs. 38 and 70) and by analyses of the intensity of the 10830 Å emission line (refs. 71 through 73). Recent mass spectrometric studies (refs. 74 through 77) also have revealed that the concentration of helium in the lower thermosphere tends to increase in the winter at high latitudes.

Through an analysis of the intensity of the 10830 Å emission line, Bitterberg et al. (ref. 78) deduced that helium varied seasonally in one year by a factor of 3 to 4 above 500 km. They pointed out that clear maxima in the helium concentration were observed repeatedly in the month of December and January and then were followed by a rather steep decline. Minima in the helium concentration were usually observed in April and May, but some early ones were observed in March.

The formation of this helium bulge over the winter pole has been explained by a seasonal subsidence of the level at which the diffusion of helium begins (refs. 68 and 79). It has been shown (ref. 38) that a change of this level by 5 km could change the amount of helium in the thermosphere by a factor of 2. However, the mechanism of this winter helium bulge and its latitudinal dependence are still under investigation.

2.2.7 Rapid Density Fluctuations Associated with Tidal and Gravity Waves

Rapid density fluctuations propagating throughout the upper atmosphere have been detected by density gauges aboard the Explorer 32 satellite (ref. 80) and by accelerometers aboard the OVI-15 satellite (ref. 81) in the altitude range from 120 to 510 km. These fluctuations are believed to be caused by tidal and gravity waves. They appear to be more prevalent at higher latitudes near the auroral region in the early morning or late evening hours and are observed to propagate mainly in a North-South direction with maximum horizontal wavelengths on the order of 130 to 520 km (ref. 80). Their vertical wavelengths increase with height. Ambient density perturbations with a half-amplitude of 50 percent from smooth density values during a short duration have been observed (ref. 80). Theoretical studies of the density variations associated with tidal and gravity waves have been conducted (refs. 82 through 89).

Because of insufficient knowledge, tidal and gravity effects have not been taken into account in the atmospheric model recommended herein.

2.3 Determination of Atmospheric Properties (90 to 2500 km)

Semi-empirical models that use empirical coefficients to correlate neutral densities with solar flux, geomagnetic activity index, time of day, and other parameters are the best engineering tools at present for predicting the atmospheric conditions encountered by a spacecraft in

Earth orbit. Examples of this kind of model are given in references 1, 2, 5, 6, 48 and 90 through 93, but those given in references 1 and 6 are the most recent ones and are the best models available now. Of these two, the model given in reference 1 has shown better results in orbital lifetime predictions than its revision given in reference 6. Therefore, the prediction method given in reference 1 is adopted in the present monograph. It should be noted, however, that the model in reference 1 is derived mainly from satellite drag data which are averaged over a considerable range in time and space. Therefore, in comparisons of model predictions with instantaneous measurements, some divergence is to be expected.

2.3.1 Analytical Method

The prediction method given in Jacchia's 1970 model (ref. 1) basically is a static diffusion model which defines temperature and chemical composition and provides densities in agreement with satellite drag observations and, to a lesser degree, with rocket probe measurements from 90 to 1100 km. In practice, densities are derived from the empirically determined temperature profile and assumed constant boundary conditions at 90 km. Mixing is assumed to prevail to an altitude of 105 km and any change in the mean molecular mass below this level is assumed to result only from dissociation of oxygen.

The distribution of mean molecular mass between 90 and 105 km is determined empirically in such a way that it results in a ratio of atomic oxygen to molecular oxygen of 1.5 at 120 km. The model also assumes that diffusive equilibrium takes place above 105 km. All of the recognized variations in the upper atmosphere as described in section 2.2 except the one associated with tidal and gravity waves are included in the model. More information on the structure of the model is given in reference 1.

A computational procedure for the prediction method is given in appendix A. The computation has been computerized and the output of the computer program gives temperature, mass density, number density, molecular mass, pressure scale height, and density scale height as functions of altitude.

2.3.2 Table Look-Up Method

A table look-up density model is provided for cases when only an estimate of atmospheric density is needed. This method eliminates the use of a computer; only a few simple hand calculations are required for computing the exospheric temperature and possibly one correction term for density if the altitude of interest is below 170 km. The accuracy of the resulting density from this simplified method should be very close to the one obtained from the analytical method except at heights where the helium becomes the predominant constituent at altitudes above 600 km.

The look-up method gives only the mass density as a function of exospheric temperature. Procedures for calculating the exospheric temperature and finding the density from this method are given in appendix B where sample problems are illustrated.

3. CRITERIA

Prediction models of the Earth's atmosphere from 90 to 2500 km for use in space vehicle design and mission planning should be obtained in accordance with section 3.1 or 3.2.

Section 3.1 should be used for predictions of density and associated atmospheric parameters; section 3.2 should be used when a quick estimate of atmospheric density is needed.

Both methods (sections 3.1 and 3.2) can be used to obtain either mean density models or models having reasonable upper density extremes. Mean density values are obtained if nominal values for predicted solar and geomagnetic activity are used for inputs; upper density values result from using plus 2σ values for predicted solar and geomagnetic activity. Table 1 gives sample predicted solar and geomagnetic data.

The upper density model obtained from the plus 2σ values, however, does not account for short term surges in geomagnetic activity, which are usually of 6 to 12 hours duration. When experiments or subsystems are considered to be sensitive to such short term effects, a geomagnetic index of 400 should be used with the predicted plus 2σ solar flux values to obtain an upper density model associated with extreme geomagnetic conditions.

3.1 Method for Predicting Density and Associated Parameters of Earth's Atmosphere (90 to 2500 km)

The prediction method given in appendix A (based on Jacchia's 1970 model) should be used to predict atmospheric density, temperature, chemical composition, molecular mass, pressure scale height, and density scale height for any time and spatial location.

Symbols, inputs, and calculation procedures are given in appendix A. Copies of the computer program for this method and the required inputs of the predicted solar and geomagnetic activity (issued monthly) are available upon request from the NASA Marshall Space Flight Center, Code S&E-AERO-Y, Huntsville, Alabama 35812.

3.2 Method for Estimating Density of Earth's Atmosphere (90 to 2500 km)

The Quick-Look Density Model given in appendix B can be used to obtain an estimate of atmospheric density for any time and spatial location. Although the Quick-Look Density Model provides density only, other atmospheric parameters may be interpolated from the tables given in reference 1 by using the exospheric temperature that is calculated by the Quick-Look Density Model.

The computation procedure of the Quick-Look Density Model is based upon the physical relationships given in appendix A, but all of the equations have been replaced by tables to eliminate the need for a computer. If interpolations are made with a three decimal accuracy, the density obtained from the Quick-Look method will be within 2 percent of that obtained by the method given in appendix A except at high altitudes above approximately 600 km where helium is the predominant constituent of the neutral gas. In this case, the prediction method given in appendix A is recommended. Otherwise, the reader is referred to reference 1 in which a simple method can be found to estimate density values at high altitudes with a correction term for helium variations.

Symbols, inputs, calculation procedures, and sample problems are given in appendix B.

TABLE 1.

AN EXAMPLE OF NOMINAL AND 2σ PREDICTIONS OF SUNSPOT NUMBERS, MEAN 10.7 SOLAR FLUX, AND GEOMAGNETIC INDEX*

(Calculation by MSFC Solar Prediction Program)

Calendar Year	Sunspot Number		Mean 10.7 cm Solar Flux		Geomagnetic Index, a_p	
	Nominal	+2σ	Nominal	+2σ	Nominal	+2σ
1968.25	107.30	119.34	153.76	165.40	13	23
1968.50	107.49	130.37	153.96	176.07	13	23
1968.75	107.74	140.40	154.18	185.77	13	23
1969.00	104.78	143.12	151.33	188.40	13	23
1969.25	103.31	147.75	149.90	192.88	13	23
1969.50	102.57	146.09	149.18	191.27	8	23
1969.75	77.64	106.36	125.07	152.85	8	23
1970.00	94.67	139.76	141.55	185.15	8	23
1970.25	90.56	128.30	137.57	174.06	8	23
1970.50	82.42	116.91	129.70	163.05	8	23
1970.75	77.64	106.36	125.07	152.85	8	23
1971.00	70.60	94.61	118.27	141.49	8	23
1971.25	62.48	85.36	111.55	132.54	8	23
1971.50	57.16	80.54	107.15	127.89	8	17
1971.75	51.17	75.38	102.21	122.39	8	17
1972.00	46.04	72.23	97.98	119.84	8	17
1972.25	42.73	70.77	95.25	118.43	8	17
1972.50	38.23	64.62	91.54	113.31	8	17
1972.75	34.02	63.08	88.07	112.04	8	17
1973.00	31.43	61.69	85.93	110.00	8	17
1973.25	27.77	57.58	84.66	107.50	8	17
1973.50	24.91	53.80	82.95	104.39	8	17
1973.75	22.37	50.18	81.42	101.40	8	17
1974.00	18.78	44.82	79.72	96.98	6	17
1974.25	16.19	41.14	77.71	93.94	6	17
1974.50	14.70	33.74	76.82	91.96	6	17
1974.75	12.31	33.04	75.39	87.26	6	17
1975.00	10.94	28.22	74.56	84.93	6	17
1975.25	10.80	24.65	74.49	82.79	6	17
1975.50	10.36	21.66	74.22	81.00	6	17
1975.75	11.76	26.13	75.06	83.68	6	17
1976.00	13.96	33.64	76.38	87.75	6	17
1976.25	17.38	44.03	78.43	96.33	6	17
1976.50	23.24	62.04	81.95	111.18	8	17
1976.75	30.81	83.81	85.42	131.05	8	23
1977.00	39.26	105.91	92.39	152.41	8	23
1977.25	48.44	123.83	99.97	169.74	8	23
1977.50	55.66	135.55	105.92	181.08	8	23
1977.75	63.86	149.23	112.68	194.30	8	23
1978.00	73.32	165.80	120.90	210.33	8	23
1978.25	81.35	178.53	128.66	222.64	8	23
1978.50	88.94	187.01	136.01	230.84	13	23
1978.75	90.88	186.67	137.88	230.51	13	23
1979.00	91.12	189.24	138.11	232.99	13	23

*These data are inferred from predicted mean sunspot numbers by linear regression techniques (ref. 94) which were modified to make quarterly predictions (ref. 95)

REFERENCES

1. Jacchia, L. G.: New Static Models of the Thermosphere and Exosphere With Empirical Temperature Profiles. Smithsonian Astrophysical Observatory Special Report No. 313, 1970.

2. Jacchia, L. G.: Static Diffusion Models of the Upper Atmosphere With Empirical Temperature Profiles. Smithsonian Contributions to Astrophysics, vol. 8, no. 9, 1965, pp. 215-257.

3. Volland, H.: A Theory of Thermospheric Dynamics – I. Diurnal and Solar Cycle Variations. Planet. Space Sci., vol. 17, 1969, pp. 1581-1597.

4. Volland, H.: A Theory of Thermospheric Dynamics – II. Geomagnetic Activity Effect, 27-day Variation and Semiannual Variation. Planet. Space Sci., vol. 17, 1969, pp. 1709-1724.

5. Weidner, D. K.; Hasseltine, C. L.; and Smith, R. E.: Models of Earth's Atmosphere (120 to 1000 km). NASA SP-8021, May 1969.

6. Jacchia, L. G.: Revised Static Models of the Thermosphere and Exosphere With Empirical Temperature Profiles. Smithsonian Astrophysical Observatory Special Report No. 332, 1971.

7. Hedin, A. E.; Mayr, H. G.; Reber, C. A.; Spencer, N. W.; and Carignan, G. R.: Empirical Model of Global Thermospheric Temperature and Composition Based on Data from the OGO-6 Quadrupole Mass Spectrometer. GSFC X-621-73-37, Goddard Space Flight Center, 1972.

8. Hinteregger, H. E.; Hall, L. A.; and Schmidtke, G.: Solar XUV Radiation and Neutral Particle Distribution in July 1963 Thermosphere. Space Research V, 1965, pp. 1175-1190.

9. Champion, K. S. W.: The Properties of the Neutral Atmosphere. Paper No. R5, presented at the Fourteenth COSPAR Meeting, June 1971.

10. Jacchia, L. G.: Solar Effects on the Acceleration of Artificial Satellites. Smithsonian Astrophysical Observatory Special Report No. 29, 1959.

11. Priester, W.; and Martin, H. A.: Solare and Tageszeitliche Effekte in der Hochatmosphare aus Beobachtungen Kunstlicher Erdsatelliten. Mitt. Univ., Sternw. Bonn, no. 29, 1960.

12. Jacchia, L. G.: A Variable Atmospheric-Density Model From Satellite Accelerations. J. Geophys. Res., vol. 65, 1960, p. 2775.

13. Jacchia, L. G.: Electromagnetic and Corpuscular Heating of the Upper Atmosphere. Space Research III, 1963, p. 3.

14. Nicolet, M.: Solar Radio Flux and Temperature of the Upper Atmosphere. J. Geophys. Res., vol. 68, 1963, p. 6121.

15. Jacchia, L. G.; and Slowey, J.: An Analysis of the Atmospheric Drag of the Explorer IX Satellite From Precisely Reduced Photographic Observations. Space Research IV, 1964, pp. 257-270.

16. Bourdeau, R. E.; Chandra, S.; and Neupert, W. M.; Time Correlation of Extreme Ultraviolet Radiation and Thermospheric Temperature. J. Geophys. Res., vol. 67, 1964, pp. 4531-4535.

17. Roemer, M.: Geomagnetic Activity Effect and 27-day Variation. Response Time of the Thermosphere and Lower Exosphere. Space Research VII, 1967, pp. 1091-1099.

18. Roemer, M.: Reaction Time of the Upper Atmosphere Within the 27-day Variation. Forschungsberichte der Astronomischen Institute, Bonn, 68-08, 1968.

19. Harris, I.; and Spencer, N. W.: The Earth's Atmosphere, in Introduction to Space Science. Edited by Hess, W. N.; and Mead, G. D. (New York: Gordon and Breach, Science Publishers), 1968, pp. 93-132.

20. Newton, G. P.: Latitudinal Dependence of the Diurnal Density Variation. J. Geophys. Res., vol. 75, 1970, pp. 5510-5516.

21. Harris, I.; and Priester, W.: Time-Dependent Structure of the Upper Atmosphere. J. Atmos. Sci., vol. 19, 1962, pp. 286-301.

22. Mahoney, J. R.: A Study of Energy Sources for the Thermosphere. Trans. Amer. Geophys. Union, vol. 47, 1966.

23. Volland, H.: A Two-Dimensional Model of the Diurnal Variation of the Thermosphere. Part I: Theory. J. Atmos. Sci., vol. 23, 1966, pp. 799-807.

24. Stubbe, P.: Simultaneous Solution of the Time Dependent Coupled Continuity Equations, Heat Conduction Equations, and Equations of Motion for a System Consisting of a Neutral Gas, an Electron Gas, and A Four Component Ion Gas. J. Atmos. and Terrest. Phys., vol. 32, 1970, pp. 865-903.

25. Volland, H.: Phase Delay Between Neutral Temperature and Neutral Density at Thermospheric Heights. J. Geophys. Res., vol. 75, 1970, pp. 5618-5620.

26. Volland, H.; and Mayr, H. G.: A Theory of the Diurnal Variations of the Thermosphere. Ann. Geophys., vol. 26, 1970, pp. 907-919.

27. King, J. W.; and Kohl, H.: Upper Atmospheric Winds and Ionospheric Drifts Caused By Neutral Air Pressure Gradients. Nature, vol. 206, 1965, pp. 699-701.

28. Lindzen, R. S.: Diurnal Velocity Oscillations in the Thermosphere. J. Geophys. Res., vol. 71, 1966, pp. 815-820.

29. Harris, I.: Horizontal Energy Transport in the Thermosphere. Trans. Amer. Geophys. Union, vol. 47, 1966, p. 459.

30. Geisler, J. E.: Atmospheric Winds in the Middle Latitude F-region. J. Atmos. Terr. Phys., vol. 28, 1966, pp. 703-730.

31. Geisler, J. E.: A Numerical Study of the Wind System in the Middle Thermosphere. Trans. Amer. Geophys. Union, vol. 48, 1967, p. 104.

32. Kohl, H.; and King, J. W.: Atmospheric Winds Between 100 and 700 km and Their Effects on the Ionosphere. J. Atmos. Terr. Phys., vol. 29, 1967, pp. 1045-1062.

33. Kohl, H.: Interactions Between Motions of the Ionized and Neutral Atmosphere at F-region Heights. Ann. IQSY, vol. 5, 1969, pp. 183-196.

34. Chandra, C.: Electron Density Distribution in the Upper F-region. J. Geophys. Res., vol. 68, 1963, pp. 1937-1942.

35. Chapman, S.: The Electrical Conductivity of the Ionosphere. Nuovo Cim., vol. 4, Suppl., 1956, pp. 1385-1412.

36. Chandra, S.; and Stubbe, P.: The Diurnal Phase Anomaly in the Upper Atmospheric Density and Temperature. Planet. Space Sci., vol. 18, 1970, pp. 1021-1033.

37. Cummack, C. H.; and Butler, P. H.: The Density Phase Anomaly in the Upper Atmosphere Density and Temperature. Planet. Space Sci., vol. 20, 1972, pp. 289-292.

38. Jacchia, L. G.; and Slowey, J. W.: Diurnal and Seasonal-Latitudinal Variations in the Upper Atmosphere. Planet. Space Sci., vol. 16, 1968, pp. 509-524.

39. Cole, K. D.: Joule Heating of the Upper Atmosphere. Austr. J. Phys., vol. 15, 1962, pp. 223-235.

40. Cole, K. D.: Electrodynamic Heating and Movement of the Thermosphere. Planet. Space Sci., vol. 19, 1971, pp. 59-75.

41. DeVries, L. L.: Experimental Evidence in Support of Joule Heating Associated with Geomagnetic Activity. NASA TMX-64568, 1971.

42. Jacchia, L. G.; Slowey, J.; and Verniani, F.: Geomagnetic Perturbations and Upper-Atmosphere Heating. J. Geophys. Res., vol. 72, 1967, pp. 1423-1434.

43. Hung, F. T.: Atmospheric Energy Change During Geomagnetic Storms. Final Report TR-793-735, Northrop-Huntsville, Huntsville, Alabama, 1970.

44. Jacchia, L. G.; and Slowey, J.: Temperature Variations in the Upper Atmosphere During Geomagnetically Quiet Intervals. J. Geophys. Res., vol. 69, 1964, pp. 4145-4148.

45. Newton, G. P.; Horowitz, R.; and Priester, W.: Atmospheric Densities From Explorer 17 Density Gauges and a Comparison with Satellite Drag Data. J. Geophys. Res., vol. 69, 1964, pp. 4690-4692.

46. Taeusch, D. R.; Carignan, G. R.; and Reber, C. A.: Neutral Composition Variation above 400 Kilometers during a Magnetic Storm. J. Geophys. Res., vol. 76, 1971, pp. 8318-8325.

47. Paetzold, H. K.; and Zschorner, H.: Bearings of Sputnik III and the Variable Acceleration of Satellites. Space Research I, 1960, pp. 24-36.

48. Paetzold, H. K.; and Zschorner, H.: The Structure of the Upper Atmosphere and Its Variations After Satellite Observations. Space Research II, 1961, pp. 958-973.

49. Cook, G. E.; and Scott, D. W.: Exospheric Densities Near Solar Minimum Derived From the Orbit of Echo 2. Planet. Space Sci., vol. 14, 1966, pp. 1149-1165.

50. King-Hele, D. G.; and Hinsgton, J.: Air Density at Heights Near 190 km in 1966-67, From The Orbit of Secor 6. Planet. Space Sci., vol. 16, 1968, pp. 675-691.

51. King-Hele, D. G.; and Walker, D. M. C.: Air Density at Heights Near 180 km in 1968 and 1969, from the Orbit of 1967-31A. Royal Aircraft Establishment, Technical Report No. 70084, 1970.

52. Cook, G. E.: The Semi-annual Variation in the Upper Atmosphere During 1967 and 1968. Planet. Space Sci., vol. 18, 1970, pp. 1573-1584.

53. Johnson, F. S.: Circulation at Ionospheric Levels. Southwest Center for Advanced Studies Report No. CWB-10531, 1964.

54. Webb, W. L.: Structure of the Stratosphere and Mesosphere (New York: Academic Press, 1966).

55. Mayr, H. G.; and Volland, H.: Semiannual Variations in the Neutral Composition. Ann. Geophys., vol. 27, 1971, pp. 513-522.

56. Jacchia, L. G.: The Semiannual Variation in the Heterosphere: A Reappraisal. Paper presented at the 14th COSPAR Meeting, Seattle, Washington, June 1971.

57. Champion, K. S. W.: Variations With Season and Latitude of Density, Temperature, and Composition in the Lower Thermosphere. Space Research VII, 1967, pp. 1101-1118.

58. Groves, G. V.: Seasonal and Latitudinal Models of Atmospheric Temperature, Pressure, and Density, 25 to 110 km. Air Force Surveys in Geophys., no. 218, 1970.

59. Marcos, F. A.; Champion, K. S. W.; and Schweinfurth, R. A.: Lower Thermosphere Density Variations in the Southern Hemisphere. Paper presented at the 14th COSPAR Plenary Meeting, Seattle, Washington, 1971.

60. Newton, G. P.; and Pelz, D. T.: Latitudinal Variations in the Neutral Atmospheric Density. J. Geophys. Res., vol. 74, 1969, p. 4109.

61. Philbrick, C. R.; and McIsaac, J. P.: Measurements of Atmospheric Composition near 400 km. Paper presented at the 14th COSPAR Plenary Meeting, Seattle, Washington, 1971.

62. Allan, R. R.: Upper-Atmospheric Heating at High Latitudes. Paper presented at the 14th COSPAR Plenary Meeting, Seattle, Washington, 1971.

63. Jacobs, R. L.: Atmospheric Density Derived From the Drag of Eleven Low Altitude Satellites. J. Geophys. Res., vol. 72, 1967, p. 1571.

64. Marcos, F. A.; Champion, K. S. W.; and Schweinfurth, R. A.: More Accelerometer and Orbital Drag Results From the SPADES (OV1-15) and Cannon Ball I (OV1-16) Satellites. Paper presented at the 13th COSPAR Plenary Meeting, Leningrad, U.S.S.R., 1970.

65. Ching, B. K.: A Note on the High-Latitude Density Bulge Inferred from Low-Altitude Satellite Drag Data. Air Force Report No. SAMSO-TR-71-329, 1971.

66. Reber, C. A.; and Nicolet, M.: Investigation of the Major Constituents of the April-May 1963 Heterosphere by the Explorer 17 Satellite. Planet. Space Sci., vol. 13, 1965, p. 617.

67. Keating, G. M.; and Prior, E. J.: Latitudinal and Seasonal Variations in Atmospheric Densities Obtained During Low Solar Activity By Means of the Inflatable Air Density Satellite. Space Research VII, 1967, p. 1119.

68. Keating, G. M.; and Prior, E. J.: The Distribution of Helium and Atomic Oxygen in the Lower Exosphere. Trans. AGU, vol. 48, 1967, p. 188.

69. Keating, G. M.; and Prior, E. J.: The Winter Helium Bulge. Space Research VIII, 1968, pp. 982-992.

70. Reber, C. A.; Cooley, J. E.; and Harpold, D. N.: Upper Atmosphere Hydrogen and Helium Measurements from the Explorer 32 Satellite. Space Research VIII, 1968, pp. 993-995.

71. Federova, N. I.: Aurorae and Airglow. Sov. Geophys. Comm. USSR Acad. Sci., vol. 13, 1967, p. 53.

72. Shefov, N. N.: Twilight Helium Emission During Low and High Geomagnetic Activity. Planet. Space Sci., vol. 16, 1968, pp. 1103-1107.

73. Tinsley, B. A.: Measurements of Twilight Helium 10830 Å Emission. Planet. Space Sci., vol. 16, 1968, pp. 91-99.

74. Hartmann, G.; Mauersberger, K.; and Muller, R.: Evaluation of the Turbopause Level From Measurements of the Helium and Argon Content of the Lower Thermosphere Above Fort Churchill. Space Research VIII, 1968, pp. 940-946.

75. Kasprzak, W. T.; Krankowsky, D.; and Nier, A. O.: A Study of Day-Night Variations in the Neutral Composition of the Lower Thermosphere. J. Geophys. Res., vol. 73, 1968, pp. 6765-6782.

76. Krankowsky, D.; Kasprzak, W. T.; and Nier, A. O.: Mass Spectrometric Studies of the Composition of the Lower Thermosphere During Summer 1967. J. Geophys. Res., vol. 73, 1968, pp. 7291-7306.

77. Muller, D.; and Hartmann, G.: A Mass Spectrometric Investigation of the Lower Thermosphere Above Fort Churchill With Special Emphasis on the Helium Content. J. Geophys. Res., vol. 74, 1969, pp. 1287-1293.

78. Bitterberg, W.; Brutchhausen, K.; Offermann, D.; and Von Zahn, U.: Lower Thermosphere Composition and Density Above Sardinia in October 1967. J. Geophys. Res., vol. 75, 1970, pp. 5528-5534.

79. Johnson, F. S.: Turbopause Processes and Effects. Space Research VII, 1967, p. 262.

80. Newton, G. P.; Pelz, D. T.; and Volland, H.: Direct in situ Measurements of Wave Propagation in the Neutral Thermosphere. J. Geophys. Res., vol. 74, 1969, pp. 183-196.

81. Champion, K. S. W.; Marcos, F. A.; and McIsaac, J. P.: Atmospheric Density Measurements By Research Satellite OV1-15. Space Research X, 1970, pp. 450-458.

82. Hines, C. O.: Internal Atmospheric Gravity Waves at Ionospheric Heights. Can. J. Phys., vol. 38, 1960, p. 1441.

83. Hines, C. O.: An Effect on Molecular Dissipation in Upper Atmospheric Gravity Waves. J. Atmospheric Terrest. Phys., vol. 30, 1968, p. 845.

84. Pitteway, M.; and Hines, C.: The Reflection and Ducting of Atmospheric Acoustic - Gravity Waves. Can. J. Phys., vol. 43, 1965, pp. 2222-2243.

85. Bretherton, F.: The Propagation of Groups of Internal Gravity Waves in a Shear Flow. Quart. J. Roy. Met. Soc., vol. 92, 1966, pp. 466-480.

86. Hines, C.; and Reddy, C.: On the Propagation of Atmospheric Gravity Waves in a Shear Flow. J. Geophys. Res., vol. 72, 1968, pp. 1015-1034.

87. Booker, J.; and Bretherton, F.: The Critical Layer for Internal Gravity Waves in a Shear Flow. J. Fluid Mech., vol. 27, 1967, pp. 513-537.

88. Volland, H.: Full Wave Calculations of Gravity Wave Propagation Through the Thermosphere. J. Geophys. Res., vol. 74, 1969, pp. 1786-1795.

89. Miller, E. B.: Atmospheric Density Variations Related to Internal Gravity Waves. NASA Contractor Report NASA CR-61359, 1971.

90. Martin, H. A.; Neveling, W.; Priester, W.; and Roemer, M.: Model of the Upper Atmosphere from 130 through 1600 km, Derived from Satellite Orbits. Space Research II, 1961, pp. 902-917.

91. Hung, F. T.; and Lou, Y. S.: Thermospheric Temperature Model Deduced From Mass Spectrometric Measurements. Northrop-Huntsville Technical Report TR-793-9-544, 1969.

92. Hung, F. T.: Thermospheric Temperature/Composition Model Deduced From Mass Spectrometric Measurements. Northrop-Huntsville Technical Report TR-793-651, 1970.

93. Weidner, D. K.; Chambers, J.; and Lou, G. Y.: A Global Model of Atmospheric Temperature, Chemical Composition, and Density (25 to 1000 km Altitude). Paper no. f. 21, presented at the 14th COSPAR Plenary Meeting, Seattle, Washington, June 1971, to be published in Space Research XII.

94. McNish, A. G.; and Lincoln, J. V.: Prediction of Sunspot Numbers. Transaction of The American Geophysical Union, vol. 30, no. 5, Oct. 1949, pp. 673-685.

95. Boykins, E. P.; and Richards, J. T.: Applications of the Lincoln-McNish Technique to the Prediction of the Remainder of the Twentieth Sunspot Cycle. Lockheed Technical Memorandum TM-54/30-89, LMSC/HREC A-782508, March 1966.

APPENDIX A
SUMMARY OF METHOD FOR COMPUTING MODEL ATMOSPHERES

The computational procedure for obtaining predicted models of the Earth's atmosphere for any time and spatial location is given below. A computer program that has been developed for this procedure is available upon request from the NASA Marshall Space Flight Center Mail Code S&E-AERO-Y, Huntsville, Alabama 35812.

Predictions of the 10.7-cm solar flux and geomagnetic activity are required as inputs. The nominal values of such data together with estimates of ± 2σ variations (95% confidence envelope) for each quarter, 10 years into the future, are issued monthly and also should be obtained from the foregoing address. Table 1 is an example of such data. The mean solar flux should be used twice, as an input for the daily (F) and 81-day mean ($\bar{F}$) solar flux.*

*In obtaining models of the Earth's atmosphere for any time in the past, observed daily and calculated 81-day mean solar flux values are used for F and $\bar{F}$.

SYMBOLS

A	Parameter used in calculating diurnal correction for exospheric temperature (equation A-11)
AV	Avogadro's number, 6.02257 x 10^{23} $mole^{-1}$
A2	Parameter used in calculating temperature for altitude greater than 125 km (equation A-17)
a_p	Geomagnetic activity index at 6.7 hours before computation time, unitless
B_j	Coefficients for calculating mean molecular mass (equation A-18), unitless
DD	Day number after Jan. 1 (input), days
DDD	Seasonal-latitudinal density correction in the lower thermosphere (equation A-20), gm/cm^3
DENJ	Mass density at geometric altitude Z with seasonal-latitudinal correction (equation A-21), gm/cm^3
DENO	Assumed mass density at lower boundary (90 km altitude), 3.46 x 10^{-9} gm/cm^3
DENS	Mass density at geometric altitude Z without seasonal-latitudinal correction, gm/cm^3
DS	Declination of Sun (equation A-6), deg
EM	Atmospheric molecular mass, unitless
F	Daily 10.7-cm solar flux (input), 10^{-22} watts/m^2/cycles/second
$\bar{F}$	81-day mean of F, ending on date atmospheric property desired (input), 10^{-22} watts/m^2/cycles/sec
FK	Universal gas constant, 8.31432 Joule/mole-°K
G	Acceleration of gravity at geometric altitude Z (equation A-19), cm/sec^2
GP	Greenwich meridian position (equation A-3), deg
HRA	Hour angle of Sun (equation A-8), deg
i	Denotes an individual constituent
J	Julian date (equation A-1), days
J*	Computed parameter used in computing GP (equation A-2), years x 100
k	Boltzmann's constant, 1.380 x 10^{-16} erg/°K
LAT	Latitude of computation point (input), deg
LNG	Longitude of computation point (input), deg

LS	Celestial longitude (equation A-5), radians
MM	Greenwich mean time from 0000 GMT(input), minutes
MO	Mean molecular mass at 90 km altitude, unitless
M(i)	Molecular mass of constituent i, unitless
N(i)	Number density of constituent i, cm^{-3}
N(TOT)	Total number density (equation A-31), cm^{-3}
N'(He)	Helium number density with seasonal-latitudinal correction, cm^{-3}
PAR	Number of particles per unit volume, cm^{-3}
Q(i)	Content of constituent i in fraction by volume, unitless
R	Parameter used in calculating diurnal correction for exospheric temperature (equation A-11), unitless
RAP	Right ascension of computation point (equation A-4), deg
RAS	Right ascension of Sun (equation A-7), deg
RE	Radius of Earth, 6.356766×10^8 cm
SH	Atmospheric pressure scale height (equation A-34), km
SP	Atmospheric density scale height (equation A-35), km
TAU	Angle between computation point and density bulge (equation A-9), deg
TC	Nighttime minimum global exospheric temperature (equation A-10), °K
TE	Exospheric temperature (equation A-14), °K
TG	Geomagnetic activity correction for exospheric temperature (equation A-12), °K
TL	Diurnal correction for exospheric temperature (equation A-11), °K
TS	Semiannual correction for exospheric temperature (equation A-13), °K
TX	Temperature at inflection point, Z=125 km (equation A-15), °K
TZ	Temperature at geometric altitude Z (equations A-16 and A-17), °K
TO	Assumed temperature at lower boundary 90 km altitude, 183 °K
T1	Parameter used in calculating temperature (equation A-16), °K/km
T3	Parameter used in calculating temperature (equation A-16), $°K/km^3$
T4	Parameter used in calculating temperature (equation A-16), $°K/km^4$
W(i)	Mass of constituent i (input), gm/mole
Y	Length of tropical year, 365.2422 days
YR	Year (input), years
η	Parameter used in calculating the diurnal correction for exospheric temperature (equation A-11), deg
θ	Parameter used in calculating the diurnal correction for exospheric temperature (equation A-11), deg

τ — Parameter used in calculating semiannual correction for exospheric temperature (equation A-13), unitless

α — Thermal diffusion coefficient for atmospheric constituent, α=-0.38 for helium, α=0 for the others, unitless

ΔHe — Semiannual correction for helium number density (equation A-29), unitless

INPUT

a_p	Geomagnetic activity index at 6.7 hours before computation time, unitless
DATE	Date, month/day/year
DD	Day number since Jan. 1, days
F	Daily 10.7 cm solar flux, used as unitless
$\bar{F}$	81-day mean of F, ending on date atmospheric properties desired, used as unitless
LAT	Latitude of computation point, north (+), south (-), deg
LNG	Longitude of computation point, east (+), west (-), deg
MM	Greenwich Mean Time from 0000 GMT, minutes
YR	Year
z	Geometric altitude, km

COMPUTATIONAL PROCEDURE

I. SUN'S DECLINATION AND HOUR ANGLE

A. Julian date (days)

$$J = 2441683 + (YR-1973) \times 365 + DD \tag{A-1}$$

where

YR = year (input)

DD = day number after January 1 (input)

B. J* parameter (years x 100)

$$J^* = \frac{J - 2415020}{36525} \tag{A-2}$$

C. Greenwich meridian position (deg)

$$GP = 99.6909833 + 36000.76854 (J^*) + 0.00038708 (J^*)^2 + 0.25068447 (MM) \tag{A-3}$$

where

MM = Greenwich mean time in minutes (input)

GP must be between 0 and 360 deg.

D. Right ascension of computation point (deg)

$$RAP = GP + LNG \tag{A-4}$$

where

LNG = longitude of computation point (input)

RAP must be between 0 and 360 degrees

E. Celestial longitude (radians)

$$LS = 0.017203 (J-2435839) + 0.0335 \sin [0.017203 (J-2435839)] - 1.410 \tag{A-5}$$

F. Declination of Sun (deg)

$$DS = \text{arc sin} \, [\sin \, (LS) \, \sin \, (23.45°)] \tag{A-6}$$

G. Right ascension of Sun (deg)

$$RAS = \text{arc sin} \left[\frac{\tan(DS)}{\tan(23.45°)} \right] \tag{A-7}$$

H. LS must be converted to degrees

I. Put RAS in quadrant of LS

J. Compute hour angle (deg)

$$HRA = RAP - RAS \tag{A-8}$$

II. TEMPERATURE COMPUTATION

A. Exospheric temperature

1. Angle between bulge and computation point (deg)

$$TAU = HRA - 37° + 6° \sin \, (HRA + 43°) \tag{A-9}$$

where

TAU must be placed between +180 and -180 degrees

2. Nighttime minimum global exospheric temperature (°K)

$$TC = 383 + 3.32 \, \bar{F} + 1.8(F-\bar{F}) \tag{A-10}$$

where

F = Daily 10.7-cm solar flux (input), 10^{-22} watts/m^2/cycle/second

$\bar{F}$ = 81-day mean of F, ending on date atmospheric property desired (input), 10^{-22} watts/m^2/cycle/second

3. Diurnal correction (°K)

$$TL = TC(1 + R \sin^{2.5} \theta) \left(1 + A \cos^{3.0} \frac{TAU}{2}\right) \tag{A-11}$$

where

$$A = R \frac{\cos^{2.5}\eta - \sin^{2.5}\theta}{1 + R \sin^{2.5}\theta}$$

$$\eta = \frac{1}{2}|LAT-DS|$$

$$\theta = \frac{1}{2}|LAT+DS|$$

LAT = latitude of computation point (input), deg

DS = Sun's declination (equation A-6), deg

$R = -0.19 + 0.25 \log_{10} \bar{F}(t - 400^d)$

$\bar{F}(t - 400^d)$ is the value of $\bar{F}$ 400 days before the computation date

4. Geomagnetic activity correction (°K)

$$TG = 1.0\, a_p + 100\, [1 - \exp(-0.08\, a_p)] \qquad \text{(A-12)}$$

where a_p is the value 6.7 hours before the computation time

5. Semiannual correction (°K)

$$TS = 2.41 + \bar{F}[0.349 + 0.206 \sin(360°\tau + 226.5°)] \sin(720°\tau + 247.6°) \qquad \text{(A-13)}$$

where

$$\tau = \frac{DD}{Y} + 0.1145 \left(\left\{ \frac{1 + \sin\left[360° \left(\frac{DD}{Y}\right) + 342.3°\right]}{2} \right\}^{2.16} - \frac{1}{2} \right)$$

Y = length of tropical year, 365.2422 days

6. Compute exospheric temperature (°K)

$$TE = TL + TG + TS \qquad \text{(A-14)}$$

B. Temperature at inflection point, Z = 125 km, (°K)

$$TX = 444.3807 + 0.02385\ TE - 392.8292 \exp(-0.0021357\ TE) \quad \text{(A-15)}$$

C. Temperature at geometric altitude levels (°K)

1. For altitude greater than 90 km but less than 125 km

$$TZ = TX + T1(Z-125) + T3(Z-125)^3 + T4(Z-125)^4 \quad \text{(A-16)}$$

where

$$T1 = 1.9 \left(\frac{TX-183}{35}\right)$$

$$T4 = 3 \left\{\frac{\left[TX - 183 - 2(T1)\left(\frac{35}{3}\right)\right]}{35^4}\right\}$$

$$T3 = -\frac{T1}{3(35)^2} + 4(T4)\left(\frac{35}{3}\right)$$

2. For altitude greater than 125 km

$$TZ = TX + (A2)\tan^{-1}\left(\frac{1}{A2}\{T1(Z-125)[1 + 4.5 \times 10^{-6} (Z-125)^{2.5}]\}\right) \quad \text{(A-17)}$$

where

$$A2 = \frac{2(TE-TX)}{\pi}$$

III. NUMBER DENSITY, MASS DENSITY, AND MOLECULAR MASS COMPUTATIONS

A. For altitude equal to or less than 105 km

1. Mean molecular mass at altitude Z (unitless)

$$EM = B_1 + B_2(Z-100) + B_3(Z-100)^2 + B_4(Z-100)^3 + B_5(Z-100)^4 + B_6(Z-100)^5 + B_7(Z-100)^6 \quad \text{(A-18)}$$

where

$B_1 = 28.15204$

$B_2 = -0.085586$

$B_3 = 1.2840 \times 10^{-4}$

$B_4 = -1.0056 \times 10^{-5}$

$B_5 = -1.0210 \times 10^{-5}$

$B_6 = 1.5044 \times 10^{-6}$

$B_7 = 9.9826 \times 10^{-8}$

2. Mass density at altitude Z before seasonal-latitudinal correction (gm/cm^3)

$$DENS=DENO \left(\frac{TO}{TZ}\right) \left(\frac{EM}{MO}\right) \exp \left[-\frac{(EM)G}{(FK)TZ}\right] \qquad \text{(A-19)}$$

where

DENO is the assumed density at 90 km altitude 3.46×10^{-9} gm/cm^3

TO is the assumed temperature at 90 km altitude 183 °K

MO is the mean molecular mass at 90 km altitude 28.82678

G is the gravity at altitude Z which can be calculated as

$$G = 980.665 \left(1 + \frac{Z}{RE}\right)^{-2} \quad (cm/sec^2)$$

RE is the radius of the Earth, 6.356766×10^3 km

FK is the universal gas constant, 8.31432 Joule/mole - °K

3. Seasonal-latitudinal correction for density (gm/cm^3)

$$DDD = 0.02(Z-90) \frac{LAT}{|LAT|} \exp [-0.045(Z-90)]$$

$$\sin^2(LAT) \sin \frac{360°}{Y} (DD + 100) \qquad \text{(A-20)}$$

4. Mass density at altitude Z with seasonal-latitudinal correction (gm/cm^3)

$$DENJ = DENS \times 10^{DDD} \tag{A-21}$$

5. Total number of particles per unit volume (cm^{-3})

$$PAR = \frac{AV(DENJ)}{EM} \tag{A-22}$$

where

AV is Avogadro's number, 6.02257×10^{23} $mole^{-1}$

6. Number density for molecular nitrogen, argon, and helium (cm^{-3})

$$N(i) = Q(i) \left(\frac{EM}{28.96}\right) PAR \tag{A-23}$$

where

i denotes N_2, Ar or He

Q(i) is the content of N_2, Ar or He (fraction by volume)

$Q(N_2) = 0.78110$

$Q(Ar) = 0.00934$

$Q(He) = 0.00001289$

7. Molecular oxygen number density (cm^{-3})

$$N(O_2) = PAR \left\{\frac{EM}{28.96} [1 + Q(O_2)]-1\right\} \tag{A-24}$$

where

$Q(O_2) = 0.20955$

8. Atomic oxygen number density (cm^{-3})

$$N(O) = 2(PAR) \left[1 - \frac{EM}{28.96}\right] \tag{A-25}$$

B. For altitude greater than 105 km

1. Hydrogen number density at 500 km altitude (cm^{-3})

$$N(H)_{500} = \text{anti log } \{73.13 - 39.4 \log (TE) + 5.5 [\log (TE)]^2\} \quad (A-26)$$

where

log denotes common logarithm

2. Hydrogen number density for altitude greater than 500 km (cm^{-3})

$$N(H) = N(H)_{500} \left(\frac{TE}{TZ}\right) \exp \left(- \frac{M(H)G}{k\ TZ}\right) \quad (A-27)$$

where

M(H) is the molecular mass of hydrogen, 1.00797

k is Boltzmann's constant, 1.380×10^{-16} erg/°K

3. Number density for molecular nitrogen, molecular and atomic oxygen, and helium (cm^{-3})

$$N(i) = N(i)_{105} \left(\frac{TE}{TZ}\right)^{(1+\alpha)} \exp \left(- \frac{M(i)G}{k\ TZ}\right) \quad (A-28)$$

where

i denotes N_2, O_2, O or He

$N(i)_{105}$ is the number density of each constituent at 105 km altitude

α is the thermal diffusion coefficient, $\alpha=-0.38$ for helium, and $\alpha=0$ for the other constituents

4. Seasonal-latitudinal correction for helium number density (unitless)

$$\Delta He = 0.5 + 1.8 \left[\left(\frac{23.45° - DS}{47.5°}\right)^{2.5} \sin^4 \left(\frac{\pi}{4} + \frac{LAT}{2}\right) + \left(\frac{23.45° + DS}{47.5°}\right)^{2.5} \sin^4 \left(\frac{\pi}{4} - \frac{LAT}{2}\right)\right] \quad (A-29)$$

5. Helium number density with seasonal-latitudinal correction (cm^{-3})

$$N'(He) = N(He)\ (\Delta He) \quad (A-30)$$

6. Total number density (cm^{-3})

$$N(TOT) = N(H) + N(He) + N(N2) + N(02) + N(0) \quad (A-31)$$

7. Mass density (gm/cm^3)

$$DENJ = N(H)\ W(H) + N(He)\ W(HE) + N(N2)\ W(N2) + N(02)\ W(02) + N(0)\ W(0) \quad (A-32)$$

where

W(i) denotes mass of constituent i in gm/mole

$W(H) = 1.6731 \times 10^{-24}$

$W(He) = 6.6435 \times 10^{-24}$

$W(N2) = 4.6496 \times 10^{-23}$

$W(02) = 5.3104 \times 10^{-23}$

$W(0) = 2.6552 \times 10^{-23}$

8. Molecular mass (unitless)

$$EM = \frac{(DENJ)\ (AV)}{N(TOT)} \quad (A-33)$$

IV. PRESSURE SCALE HEIGHT (km)

$$SH = \frac{8.31432 \times 10^{-3}\ (TZ)}{(EM)\ (G)} \quad (A-34)$$

V. DENSITY SCALE HEIGHT (km)

$$SP = \frac{8.31432 \times 10^{-3}\ (TZ)/(EM)\ (G)}{1 + \frac{8.31432}{G} \times 10^{-3} \frac{d}{dZ}\left[\frac{TZ}{EM}\right]} \quad (A-35)$$

OUTPUT

Temperature, °K

Number density of N_2, O_2, O, He, and H, cm^{-3}

Total number density, cm^{-3}

Mass density, gm/cm^3

Molecular mass, unitless

Pressure scale height, km

Density scale height, km

APPENDIX B
QUICK-LOOK DENSITY MODEL WITH SAMPLE PROBLEMS

The computational procedure and sample problems for obtaining an estimate of atmospheric density for a given time and location are given below. Required inputs include predictions of the 10.7-cm solar flux and geomagnetic activity for the future time desired. Such data are issued monthly and current predictions should be obtained from the NASA Marshall Space Flight Center, Code S&E-AERO-Y, Huntsville, Alabama 35812.

SYMBOLS

a_p	Geomagnetic activity index at 6.7 hours before computation time, unitless
DS	Declination of Sun, deg
F	Daily 10.7-cm solar flux, 10^{-22} watts/m^2/cycles/second
$\bar{F}$	81-day mean of F, ending on date atmospheric property desired, 10^{-22} watts/m^2/cycle/second
$\bar{F}(t-400^d)$	Value of $\bar{F}$ 400 days before computation time, 10^{-22} watts/m^2/cycle/second
LAT	Latitude of computation point, deg
P	Parameter used for computing seasonal-latitudinal density correction in the lower thermosphere (Table B-4), unitless
R	Parameter used in calculating diurnal correction for exospheric temperature (equation A-11), unitless
S	Parameter used for computing seasonal-latitudinal density correction in the lower thermosphere (Table B-4), gm/cm^3
TC	Nighttime minimum global exospheric temperature (equation A-10), °K
TE	Exospheric temperature (equation A-14), °K
TG	Geomagnetic activity correction for exospheric temperature (equation A-12), °K
TL	Diurnal correction for exospheric temperature (equation A-11), °K
TS	Semiannual correction for exospheric temperature (equation A-13), °K

Z	Geometric height, km
ρ	Mass density, gm/cm^3
δT_s	Parameter used for computing semiannual correction of exospheric temperature (Table B-3), °K

INPUT*

DATE	Date, month/day/year (January 1, 1975)
F	Daily 10.7-cm solar flux (74.56)
$\bar{F}$	81-day mean solar flux (74.56)
$\bar{F}(t-400^d)$	Value of $\bar{F}$ 400 days before computation time (80.8)
a_p	Geomagnetic activity index (6)
LAT	Latitude of computation point (45°N)
LT	Local time (1000)
Z	Altitude of interest (130 and 400 km)

COMPUTATIONAL PROCEDURE AND SAMPLE PROBLEMS

The following examples illustrate the step-by-step procedure for obtaining an estimate of the atmospheric density over a point with geographic latitude 45°N on January 1, 1975, at 1000 hours local time, for two heights: Z = 130 km and Z = 400 km. From the sample data in table 1, the predicted nominal geomagnetic and mean solar flux indices are found to be 6 and 74.56, respectively. The geomagnetic index from table 1 is used as the value occurring 6.7 hours before the computation time; and the mean solar flux is used twice, as the 81-day mean of 10.7-cm solar flux and the actual flux on the day before.** It should be noted, however, that table 1 is only a sample; the most recent predictions of the 10.7-cm solar flux and geomagnetic activity should be obtained for predicting atmospheric density.

*Inputs for sample problems in parenthesis.

**In obtaining models of the Earth's atmosphere for any time in the past, observed daily and calculated 81-day mean solar flux values are used for F and $\bar{F}$, and the observed value of geomagnetic activity index at 6.7 hours before the computation time is used for a_p.

I. EXOSPHERIC TEMPERATURE COMPUTATION

A. Nighttime minimum global exospheric temperature (equation A-10)

$$TC = 383 + 3.32\ \bar{F} + 1.8(F-\bar{F})$$

$$= 383 + 3.32 \times 74.56 + 1.8(74.56-74.56)$$

$$= 630.5\ ^\circ K$$

B. Exospheric temperature with diurnal correction

1. From Figure B-1, the declination of the Sun on January 1 is

$$DS = -23.45^\circ$$

2. For LAT = +45° and local time = 1000, Table B-1 gives TL/TC = 1.116 However, Table B-1 is computed for R=0.31. The actual R, according to equation A-11, is

$$R = -0.19 + 0.25 \log_{10} \bar{F}(t-400^d)$$

$$= -0.19 + 0.25 \log_{10} (80.8)$$

$$= 0.287$$

where

$\bar{F}(t-400^d)$ is obtained from Table 1.

3. Therefore, the exospheric temperature with diurnal correction is

$$TL = 630.5 \times 1.116 \left[1 - \left(\frac{0.31 - 0.287}{0.31}\right)\right]$$

$$= 630.5 \times 1.033$$

$$= 651.3\ ^oK$$

C. Geomagnetic activity correction

From Table B-2, for a_p=6, we find

$$TG = +47\ ^\circ K$$

D. Semiannual correction

From Table B-3, for January 1, we have

$$\delta T_s = -11.6 \text{ °K}$$

Therefore, the semiannual correction is

$$TS = \frac{\bar{F}}{100} \delta T_s$$

$$= 0.7456 \ (-11.6)$$

$$= -8.6 \text{ °K}$$

E. Exospheric temperature (equation A-4)

$$TE = TL + TG + TS$$

$$= 651.3 + 47 - 8.6$$

$$= 689.7 \text{ °K}$$

II. ATMOSPHERIC DENSITY INTERPOLATIONS

TE, which is the final exospheric temperature, should be used to enter Table B-5 to obtain the atmospheric density at any desired altitude.

A. Density at Z=130 km

1. From Table B-5, for TE = 689.7 °K, we have $\log_{10} \rho = -11.121$
2. For seasonal-latitudinal correction, we use Table B-4 where

$$S = 0.132, \ P = 0.989, \ \sin^2(\text{LAT}) = 0.500$$

Therefore,

$$\Delta \log_{10} \rho = (S)\ (P)\ \sin^2\ (\text{LAT})$$

$$= 0.065$$

3. Final density at Z = 130 km

$$\log_{10} \rho = -11.121 + 0.065$$

$$= -11.056$$

or

$$\rho = 10^{-11.056} \text{ gm/cm}^3$$

B. Density at Z = 400 km

From Table B-5, for TE = 689.8 ^oK, we have

$$\log_{10}\rho = -15.285$$

or

$$\rho = 10^{-15.285} \text{ gm/cm}^3$$

At this height the seasonal-latitudinal correction for density, according to Table B-4, is negligible.

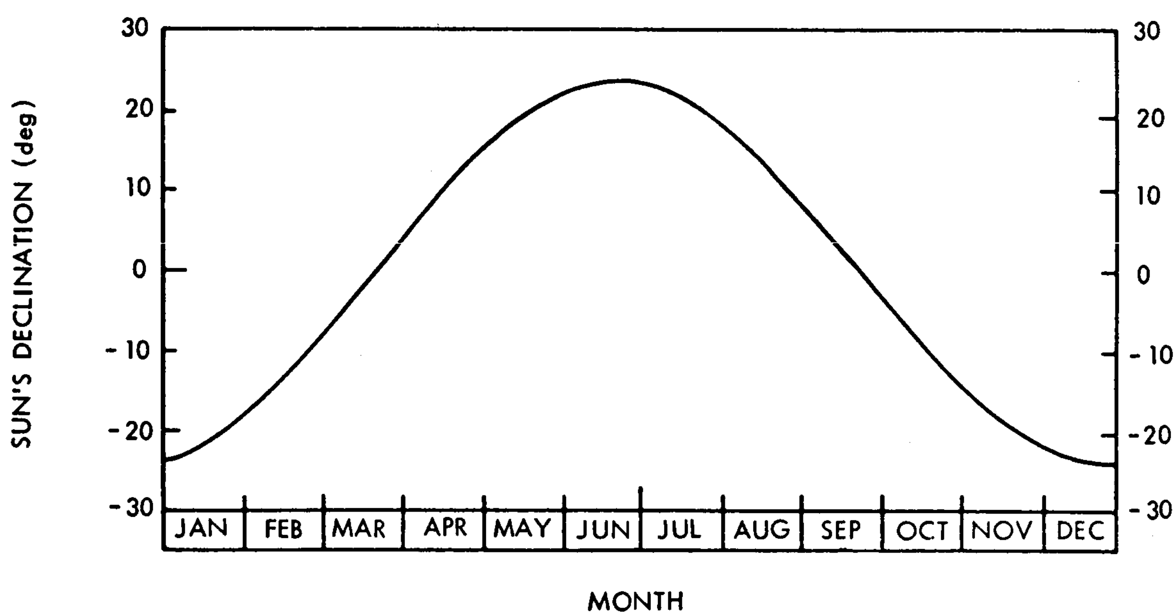

Figure B-1. DECLINATION OF SUN

TABLE B-1

RATIO OF THE LOCAL TEMPERATURE (TL) TO THE GLOBAL MINIMUM TEMPERATURE (TC) AS A FUNCTION OF LOCAL TIME AND OF LATITUDE (LAT). ALL RATIOS HAVE BEEN MULTIPLIED BY 1000 TO ELIMINATE THE DECIMAL POINT (AFTER REF. 1).

DS = +23°44

LAT (deg)	LOCAL TIME (hr)																							
	0	1	2	3	4	5	6	7	8	9	10	11	12	13	14	15	16	17	18	19	20	21	22	23
90	1198	1198	1198	1198	1198	1198	1198	1198	1198	1198	1198	1198	1198	1198	1198	1198	1198	1198	1198	1198	1198	1198	1198	1198
75	1158	1156	1155	1155	1155	1157	1161	1168	1178	1191	1204	1218	1229	1236	1239	1237	1231	1222	1211	1200	1188	1178	1170	1163
60	1119	1114	1112	1112	1113	1116	1123	1137	1156	1181	1207	1233	1253	1267	1272	1269	1258	1241	1220	1198	1177	1157	1140	1128
45	1083	1076	1074	1074	1074	1079	1089	1108	1135	1169	1206	1241	1270	1289	1296	1292	1276	1253	1224	1193	1163	1136	1113	1095
30	1054	1045	1042	1042	1043	1048	1061	1083	1116	1156	1200	1243	1277	1300	1309	1303	1284	1256	1222	1185	1150	1117	1089	1068
15	1032	1023	1020	1019	1020	1026	1039	1064	1099	1143	1191	1236	1274	1299	1308	1301	1281	1251	1214	1174	1136	1100	1070	1047
0	1018	1009	1006	1006	1007	1012	1026	1050	1085	1129	1177	1223	1260	1285	1294	1288	1268	1237	1200	1161	1122	1087	1057	1034
-15	1012	1004	1001	1000	1001	1006	1019	1042	1074	1115	1160	1202	1237	1260	1269	1263	1244	1216	1181	1145	1109	1076	1048	1027
-30	1010	1003	1001	1000	1001	1005	1017	1036	1065	1100	1139	1176	1206	1226	1234	1229	1212	1188	1158	1126	1094	1066	1042	1023
-45	1013	1007	1005	1005	1005	1009	1018	1034	1057	1085	1116	1146	1171	1187	1193	1189	1176	1156	1132	1106	1080	1057	1038	1023
-60	1023	1019	1017	1017	1018	1020	1026	1037	1054	1074	1095	1116	1134	1145	1149	1146	1137	1123	1106	1088	1070	1054	1040	1030
-75	1042	1040	1039	1039	1039	1040	1043	1049	1057	1068	1079	1090	1099	1105	1107	1105	1101	1093	1085	1075	1066	1058	1051	1045
-90	1069	1069	1069	1069	1069	1069	1069	1069	1069	1069	1069	1069	1069	1069	1069	1069	1069	1069	1069	1069	1069	1069	1069	1069

DS = +20°

LAT (deg)	LOCAL TIME (hr)																							
	0	1	2	3	4	5	6	7	8	9	10	11	12	13	14	15	16	17	18	19	20	21	22	23
90	1188	1188	1188	1188	1188	1188	1188	1188	1188	1188	1188	1188	1188	1188	1188	1188	1188	1188	1188	1188	1188	1188	1188	1188
75	1148	1146	1145	1145	1145	1147	1151	1158	1168	1181	1195	1209	1220	1227	1230	1228	1222	1213	1202	1190	1179	1169	1160	1153
60	1110	1105	1103	1103	1103	1106	1114	1128	1148	1172	1199	1225	1246	1260	1265	1262	1250	1233	1212	1190	1168	1148	1132	1119
45	1075	1069	1066	1066	1066	1071	1081	1100	1128	1162	1200	1236	1265	1285	1292	1287	1271	1247	1218	1187	1157	1129	1106	1088
30	1048	1039	1036	1036	1037	1042	1055	1078	1111	1152	1197	1240	1275	1298	1307	1301	1282	1254	1219	1182	1145	1112	1084	1062
15	1028	1019	1016	1015	1016	1022	1036	1061	1096	1141	1190	1236	1275	1300	1309	1303	1282	1251	1214	1173	1134	1098	1067	1044
0	1017	1008	1004	1004	1005	1010	1024	1049	1085	1130	1179	1225	1264	1289	1298	1292	1271	1240	1203	1162	1123	1087	1056	1033
-15	1012	1004	1000	1000	1001	1006	1019	1043	1076	1118	1163	1207	1243	1266	1275	1269	1250	1221	1186	1148	1111	1077	1049	1027
-30	1011	1004	1001	1001	1001	1006	1018	1038	1067	1104	1144	1182	1214	1235	1242	1237	1220	1195	1164	1131	1098	1069	1044	1024
-45	1015	1009	1007	1007	1007	1011	1020	1037	1061	1091	1123	1154	1179	1196	1202	1198	1185	1164	1139	1112	1086	1062	1041	1026
-60	1027	1023	1021	1021	1022	1024	1031	1042	1059	1080	1103	1125	1143	1155	1159	1156	1147	1132	1114	1095	1077	1060	1046	1035
-75	1048	1046	1045	1045	1045	1047	1050	1056	1065	1075	1087	1099	1108	1114	1116	1115	1110	1102	1093	1083	1074	1065	1058	1052
-90	1077	1077	1077	1077	1077	1077	1077	1077	1077	1077	1077	1077	1077	1077	1077	1077	1077	1077	1077	1077	1077	1077	1077	1077

TABLE B-1. (continued)

DS = 10°

LAT (deg)	LOCAL TIME (hr) 0	1	2	3	4	5	6	7	8	9	10	11	12	13	14	15	16	17	18	19	20	21	22	23
90	1159	1159	1159	1159	1159	1159	1159	1159	1159	1159	1159	1159	1159	1159	1159	1159	1159	1159	1159	1159	1159	1159	1159	1159
75	1120	1117	1116	1116	1117	1118	1122	1130	1140	1153	1167	1181	1192	1200	1202	1201	1195	1186	1174	1163	1151	1140	1132	1125
60	1084	1079	1077	1077	1078	1081	1089	1103	1123	1148	1175	1201	1223	1237	1242	1239	1227	1210	1189	1166	1144	1124	1107	1093
45	1055	1048	1045	1045	1046	1050	1061	1080	1109	1144	1182	1218	1248	1268	1275	1270	1254	1230	1200	1169	1138	1110	1086	1067
30	1033	1025	1022	1021	1022	1027	1041	1064	1098	1140	1186	1230	1266	1289	1298	1292	1273	1244	1208	1170	1133	1099	1070	1048
15	1020	1011	1007	1007	1008	1014	1028	1053	1090	1136	1186	1234	1274	1300	1309	1303	1282	1250	1211	1169	1129	1092	1060	1036
0	1014	1005	1001	1001	1002	1008	1022	1048	1085	1132	1182	1231	1271	1297	1307	1300	1279	1247	1207	1165	1124	1087	1055	1031
-15	1013	1004	1001	1000	1001	1007	1020	1045	1081	1125	1173	1220	1258	1283	1292	1285	1265	1234	1197	1157	1118	1082	1052	1029
-30	1015	1007	1004	1004	1005	1010	1022	1044	1076	1116	1159	1200	1235	1257	1265	1260	1241	1214	1180	1145	1109	1077	1050	1029
-45	1025	1018	1016	1015	1016	1020	1030	1048	1075	1107	1143	1177	1204	1223	1230	1225	1210	1187	1160	1131	1102	1076	1053	1036
-60	1043	1038	1036	1036	1036	1039	1047	1059	1078	1101	1126	1150	1170	1183	1188	1185	1174	1158	1139	1118	1097	1079	1063	1051
-75	1069	1067	1066	1066	1066	1067	1071	1078	1087	1099	1113	1125	1135	1142	1145	1143	1137	1129	1119	1108	1097	1088	1080	1073
-90	1103	1103	1103	1103	1103	1103	1103	1103	1103	1103	1103	1103	1103	1103	1103	1103	1103	1103	1103	1103	1103	1103	1103	1103

DS = 0°

LAT (deg)	LOCAL TIME (hr) 0	1	2	3	4	5	6	7	8	9	10	11	12	13	14	15	16	17	18	19	20	21	22	23
90	1130	1130	1130	1130	1130	1130	1130	1130	1130	1130	1130	1130	1130	1130	1130	1130	1130	1130	1130	1130	1130	1130	1130	1130
75	1093	1091	1090	1090	1090	1092	1096	1103	1113	1126	1140	1153	1164	1171	1174	1172	1166	1157	1146	1135	1124	1113	1105	1098
60	1062	1057	1055	1055	1055	1058	1066	1080	1099	1124	1151	1176	1197	1211	1216	1213	1202	1185	1164	1142	1120	1100	1083	1071
45	1038	1031	1028	1028	1029	1033	1044	1063	1091	1125	1162	1198	1228	1247	1254	1249	1234	1210	1181	1150	1119	1092	1068	1050
30	1022	1014	1011	1011	1011	1017	1030	1053	1086	1128	1173	1216	1252	1275	1284	1278	1259	1230	1195	1158	1121	1087	1059	1037
15	1015	1006	1002	1002	1003	1009	1023	1048	1085	1131	1181	1229	1268	1294	1303	1297	1276	1244	1205	1164	1123	1087	1055	1031
0	1013	1004	1000	1000	1001	1007	1022	1048	1086	1133	1184	1233	1273	1300	1310	1303	1282	1249	1209	1167	1125	1087	1055	1030
-15	1015	1006	1002	1002	1003	1009	1023	1048	1085	1131	1181	1229	1268	1294	1303	1297	1276	1244	1205	1164	1123	1087	1055	1031
-30	1022	1014	1011	1011	1011	1017	1030	1053	1086	1129	1173	1216	1252	1275	1284	1278	1259	1230	1195	1158	1121	1087	1059	1037
-45	1038	1031	1028	1028	1029	1033	1044	1063	1091	1125	1162	1198	1228	1247	1254	1249	1234	1210	1181	1150	1119	1092	1068	1050
-60	1062	1057	1055	1055	1055	1058	1066	1080	1099	1124	1151	1176	1197	1211	1216	1213	1202	1185	1164	1142	1120	1100	1083	1071
-75	1093	1091	1090	1090	1090	1092	1096	1103	1113	1126	1140	1153	1164	1171	1174	1172	1166	1157	1146	1135	1124	1113	1105	1098
-90	1130	1130	1130	1130	1130	1130	1130	1130	1130	1130	1130	1130	1130	1130	1130	1130	1130	1130	1130	1130	1130	1130	1130	1130

DS = -10°

LAT (deg)	LOCAL TIME (hr) 0	1	2	3	4	5	6	7	8	9	10	11	12	13	14	15	16	17	18	19	20	21	22	23
90	1103	1103	1103	1103	1103	1103	1103	1103	1103	1103	1103	1103	1103	1103	1103	1103	1103	1103	1103	1103	1103	1103	1103	1103
75	1069	1067	1066	1066	1066	1067	1071	1078	1087	1099	1113	1125	1135	1142	1145	1143	1137	1129	1119	1108	1097	1088	1080	1073
60	1043	1038	1036	1036	1036	1039	1047	1059	1078	1101	1126	1150	1170	1183	1188	1185	1174	1158	1139	1118	1097	1079	1063	1051
45	1025	1018	1016	1015	1016	1020	1030	1048	1075	1107	1143	1177	1204	1223	1230	1225	1210	1187	1160	1131	1102	1076	1053	1036
30	1015	1007	1004	1004	1005	1010	1022	1044	1076	1116	1159	1200	1235	1257	1265	1260	1241	1214	1180	1145	1109	1077	1050	1029
15	1013	1004	1001	1000	1001	1007	1020	1045	1081	1125	1173	1220	1258	1283	1292	1285	1265	1234	1197	1157	1118	1082	1052	1029
0	1014	1005	1001	1001	1002	1008	1022	1048	1085	1132	1182	1231	1271	1297	1307	1300	1279	1247	1207	1165	1124	1087	1055	1031
-15	1020	1011	1007	1007	1008	1014	1028	1053	1090	1136	1186	1234	1274	1300	1309	1303	1282	1250	1211	1169	1129	1092	1060	1036
-30	1033	1025	1022	1021	1022	1027	1041	1064	1098	1140	1186	1230	1266	1289	1298	1292	1273	1244	1208	1170	1133	1099	1070	1048
-45	1055	1048	1045	1045	1046	1050	1061	1080	1109	1144	1182	1218	1248	1268	1275	1270	1254	1230	1200	1169	1138	1110	1086	1067
-60	1084	1079	1077	1077	1078	1081	1089	1103	1123	1148	1175	1201	1223	1237	1242	1239	1227	1210	1189	1166	1144	1124	1107	1093
-75	1120	1117	1116	1116	1117	1118	1122	1130	1140	1153	1167	1181	1192	1200	1202	1201	1195	1186	1174	1163	1151	1140	1132	1125
-90	1159	1159	1159	1159	1159	1159	1159	1159	1159	1159	1159	1159	1159	1159	1159	1159	1159	1159	1159	1159	1159	1159	1159	1159

TABLE B-1. (concluded)

DS = -20°

LAT (deg)	LOCAL TIME (hr)																							
	0	1	2	3	4	5	6	7	8	9	10	11	12	13	14	15	16	17	18	19	20	21	22	23
90	1077	1077	1077	1077	1077	1077	1077	1077	1077	1077	1077	1077	1077	1077	1077	1077	1077	1077	1077	1077	1077	1077	1077	1077
75	1048	1046	1045	1045	1045	1047	1050	1056	1065	1075	1087	1099	1108	1114	1116	1115	1110	1102	1093	1083	1074	1065	1058	1052
60	1027	1023	1021	1021	1022	1024	1031	1042	1059	1080	1103	1125	1143	1155	1159	1156	1147	1132	1114	1095	1077	1060	1046	1035
45	1015	1009	1007	1007	1007	1011	1020	1037	1061	1091	1123	1154	1179	1196	1202	1198	1185	1164	1139	1112	1086	1062	1041	1026
30	1011	1004	1001	1001	1001	1006	1018	1038	1067	1104	1144	1182	1214	1235	1242	1237	1220	1195	1164	1131	1098	1069	1044	1024
15	1012	1004	1000	1000	1001	1006	1019	1043	1076	1118	1163	1207	1243	1266	1275	1269	1250	1221	1186	1148	1111	1077	1049	1027
0	1017	1008	1004	1004	1005	1010	1024	1049	1085	1130	1179	1225	1264	1289	1298	1292	1271	1240	1203	1162	1123	1087	1056	1033
-15	1028	1019	1016	1015	1016	1022	1036	1061	1096	1141	1190	1236	1275	1300	1309	1303	1282	1251	1214	1173	1134	1098	1067	1044
-30	1048	1039	1036	1036	1037	1042	1055	1078	1111	1152	1197	1240	1275	1298	1307	1301	1282	1254	1219	1182	1145	1112	1084	1062
-45	1075	1069	1066	1066	1066	1071	1081	1100	1128	1162	1200	1236	1265	1285	1292	1287	1271	1247	1218	1187	1157	1129	1106	1088
-60	1110	1105	1103	1103	1103	1106	1114	1128	1148	1172	1199	1225	1246	1260	1265	1262	1250	1233	1212	1190	1168	1148	1132	1119
-75	1148	1146	1145	1145	1145	1147	1151	1158	1168	1181	1195	1209	1220	1227	1230	1228	1222	1213	1202	1190	1179	1169	1160	1153
-90	1188	1188	1188	1188	1188	1188	1188	1188	1188	1188	1188	1188	1188	1188	1188	1188	1188	1188	1188	1188	1188	1188	1188	1188

DS = -23°44

LAT (deg)	LOCAL TIME (hr)																							
	0	1	2	3	4	5	6	7	8	9	10	11	12	13	14	15	16	17	18	19	20	21	22	23
90	1069	1069	1069	1069	1069	1069	1069	1069	1069	1069	1069	1069	1069	1069	1069	1069	1069	1069	1069	1069	1069	1069	1069	1069
75	1042	1040	1039	1039	1039	1040	1043	1049	1057	1068	1079	1090	1099	1105	1107	1105	1101	1093	1085	1075	1066	1058	1051	1045
60	1023	1019	1017	1017	1018	1020	1026	1037	1054	1074	1095	1116	1134	1145	1149	1146	1137	1123	1106	1088	1070	1054	1040	1030
45	1013	1007	1005	1005	1005	1009	1018	1034	1057	1085	1116	1146	1171	1187	1193	1189	1176	1156	1132	1106	1080	1057	1038	1023
30	1010	1003	1001	1000	1001	1005	1017	1036	1065	1100	1139	1176	1206	1226	1234	1229	1212	1188	1158	1126	1094	1066	1042	1023
15	1012	1004	1001	1000	1001	1006	1019	1042	1074	1115	1160	1202	1237	1260	1269	1263	1244	1216	1181	1145	1109	1076	1048	1027
0	1018	1009	1006	1006	1007	1012	1026	1050	1085	1129	1177	1223	1260	1285	1294	1288	1268	1237	1200	1161	1122	1087	1057	1034
-15	1032	1023	1020	1019	1020	1026	1039	1064	1099	1143	1191	1236	1274	1299	1308	1301	1281	1251	1214	1174	1136	1100	1070	1047
-30	1054	1045	1042	1042	1043	1048	1061	1083	1116	1156	1200	1243	1277	1300	1309	1303	1284	1256	1222	1185	1150	1117	1089	1068
-45	1083	1076	1074	1074	1074	1079	1089	1108	1135	1169	1206	1241	1270	1289	1296	1292	1276	1253	1224	1193	1163	1136	1113	1095
-60	1119	1114	1112	1112	1113	1116	1123	1137	1156	1181	1207	1233	1253	1267	1272	1269	1258	1241	1220	1198	1177	1157	1140	1128
-75	1158	1156	1155	1155	1155	1157	1161	1168	1178	1191	1204	1218	1229	1236	1239	1237	1231	1222	1211	1200	1188	1178	1170	1163
-90	1198	1198	1198	1198	1198	1198	1198	1198	1198	1198	1198	1198	1198	1198	1198	1198	1198	1198	1198	1198	1198	1198	1198	1198

TABLE B-2.

TEMPERATURE INCREMENT AS A FUNCTION OF GEOMAGNETIC INDICES (AFTER REF. 1)

a_p	TG (°K)	a_p	TG (°K)
0	0	39	134
2	9	48	145
3	19	56	156
4	28	67	167
5	37	80	180
6	47	94	194
7	56	111	210
9	66	132	229
12	75	154	251
15	85	179	279
18	94	207	313
22	104	236	358
27	114	300	417
32	124	400	495

TABLE B-3.

TEMPERATURE CORRECTIONS δT_s FOR THE SEMIANNUAL VARIATION,* COMPUTED FROM EQUATION A-13, FOR $\bar{F}_{10.7}$ = 100 (AFTER REF. 1)

DATE	δT_s (°K)	DATE	δT_s (°K)
Jan. 1	-11°.6	July 9	-43°.6
11	-15.6	19	-47.9
21	-15.4	29	-50.1
31	-11.9	Aug. 8	-48.8
Feb. 10	- 6.5	18	-42.9
20	+ 0.1	28	-31.9
March 2	+ 7.8	Sept. 7	-16.4
12	+16.2	17	+ 1.7
22	+23.5	27	+19.7
April 1	+27.5	Oct. 7	+34.9
11	+26.7	17	+45.1
21	+21.1	27	+49.0
May 1	+12.5	Nov. 6	+46.7
11	+ 2.7	16	+39.2
21	- 7.1	26	+28.0
31	-16.0	Dec. 6	+15.1
June 10	-24.1	16	+ 2.5
20	-31.3	26	- 7.7
30	-37.8		

*The actual correction is $\Delta TS = \frac{\bar{F}_{10.7}}{100}\,\delta T_s$.

TABLE B-4.

TABLES FOR THE SEASONAL-LATITUDINAL DENSITY VARIATION (AFTER REF. 1) $\Delta \text{LOG } \rho = (S)(P) \sin^2 (\text{LAT})$

TABLE OF THE MAXIMUM AMPLITUDE, $S = 0.02 (Z - 90) \exp [-0.045 (Z - 90)]$

Z (km)	S	Z (km)	S	Z (km)	S
90	0. 000	130	0. 132	200	0. 016
95	0. 080	140	0. 105	220	0. 007
100	0. 128	150	0. 081	240	0. 004
105	0. 153	160	0. 060	260	0. 001
110	0. 163	170	0. 044	280	0. 001
115	0. 162	180	0. 031	300	0. 000
120	0. 156	190	0. 022		

TABLE OF THE PHASE, $P = \sin \frac{360^\circ}{Y} (d + 100)$*

DATE	P	DATE	P	DATE	P	DATE	P
Jan. 1	±0. 989	Apr. 1	∓0. 129	June 30	∓0. 994	Sept. 28	±0. 086
11	±0. 948	11	∓0. 297	July 10	∓0. 961	Oct. 8	±0. 255
21	±0. 880	21	∓0. 456	20	∓0. 900	18	±0. 417
31	±0. 786	May 1	∓0. 602	30	∓0. 812	20	±0. 567
Feb. 10	±0. 668	11	∓0. 730	Aug. 9	∓0. 699	Nov. 7	±0. 699
20	±0. 531	21	∓0. 836	19	∓0. 567	17	±0. 812
Mar. 2	±0. 378	31	∓0. 918	29	∓0. 417	27	±0. 900
12	±0. 214	June 10	∓0. 972	Sept. 8	∓0. 255	Dec. 7	±0. 961
22	±0. 043	20	∓0. 998	18	∓0. 086	17	±0. 994
Apr. 1	∓0. 129	30	∓0. 994	28	±0. 086	27	±0. 998

*Take the upper sign for the Northern Hemisphere, the lower for the Southern Hemisphere.

TABLE OF $\sin^2$ (LAT)

LAT	$\sin^2$ (LAT)	LAT	$\sin^2$ (LAT)	LAT	$\sin^2$ (LAT)
0°	0. 000	30°	0. 250	60°	0. 750
5	0. 008	35	0. 329	65	0. 821
10	0. 030	40	0. 413	70	0. 883
15	0. 067	45	0. 500	75	0. 933
20	0. 117	50	0. 587	80	0. 970
25	0. 179	55	0. 671	85	0. 992
30	0. 250	60	0. 750	90	1. 000

TABLE B-5.

ATMOSPHERIC DENSITY AS A FUNCTION OF HEIGHT AND EXOSPHERIC TEMPERATURE (DECIMAL LOGARITHMS, g/cm^3) (AFTER REF. 1)

ALTITUDE (km)	EXOSPHERIC TEMPERATURE (°K) 600	650	700	750	800	850	900	950	1000	1050
90	-8.461	-8.461	-8.461	-8.461	-8.461	-8.461	-8.461	-8.461	-8.461	-8.461
92	-8.620	-8.620	-8.620	-8.620	-8.620	-8.620	-8.620	-8.620	-8.620	-8.620
94	-8.779	-8.779	-8.780	-8.780	-8.780	-8.780	-8.780	-8.780	-8.780	-8.780
96	-8.939	-8.940	-8.940	-8.940	-8.940	-8.941	-8.941	-8.941	-8.941	-8.941
98	-9.099	-9.100	-9.100	-9.101	-9.101	-9.101	-9.102	-9.102	-9.102	-9.102
100	-9.258	-9.259	-9.259	-9.260	-9.261	-9.261	-9.262	-9.262	-9.262	-9.263
102	-9.415	-9.416	-9.417	-9.418	-9.418	-9.419	-9.420	-9.420	-9.421	-9.421
104	-9.570	-9.571	-9.572	-9.573	-9.574	-9.574	-9.575	-9.575	-9.576	-9.576
106	-9.722	-9.723	-9.724	-9.725	-9.725	-9.726	-9.726	-9.727	-9.727	-9.728
108	-9.870	-9.871	-9.871	-9.872	-9.872	-9.873	-9.873	-9.873	-9.874	-9.874
110	-10.014	-10.014	-10.014	-10.014	-10.014	-10.015	-10.015	-10.015	-10.015	-10.015
115	-10.350	-10.348	-10.346	-10.345	-10.344	-10.343	-10.342	-10.341	-10.340	-10.339
120	-10.650	-10.645	-10.641	-10.637	-10.634	-10.631	-10.628	-10.626	-10.624	-10.622
125	-10.914	-10.905	-10.897	-10.891	-10.885	-10.880	-10.876	-10.872	-10.868	-10.865
130	-11.143	-11.130	-11.119	-11.109	-11.101	-11.094	-11.087	-11.081	-11.076	-11.072
135	-11.340	-11.324	-11.309	-11.297	-11.286	-11.277	-11.269	-11.261	-11.255	-11.249
140	-11.513	-11.492	-11.475	-11.460	-11.447	-11.436	-11.426	-11.417	-11.410	-11.403
145	-11.667	-11.642	-11.622	-11.604	-11.589	-11.576	-11.564	-11.554	-11.546	-11.538
150	-11.808	-11.779	-11.755	-11.734	-11.717	-11.701	-11.689	-11.677	-11.667	-11.659
155	-11.940	-11.906	-11.878	-11.854	-11.834	-11.817	-11.802	-11.789	-11.778	-11.768
160	-12.064	-12.025	-11.993	-11.966	-11.943	-11.923	-11.907	-11.892	-11.880	-11.869
170	-12.296	-12.248	-12.207	-12.172	-12.143	-12.119	-12.098	-12.080	-12.064	-12.051
180	-12.512	-12.453	-12.404	-12.362	-12.327	-12.297	-12.271	-12.249	-12.230	-12.213
190	-12.714	-12.645	-12.588	-12.539	-12.498	-12.462	-12.431	-12.405	-12.382	-12.362
200	-12.904	-12.827	-12.762	-12.706	-12.658	-12.617	-12.582	-12.551	-12.524	-12.501
210	-13.085	-13.000	-12.927	-12.864	-12.811	-12.764	-12.724	-12.689	-12.658	-12.632
220	-13.258	-13.164	-13.084	-13.015	-12.956	-12.904	-12.859	-12.820	-12.786	-12.755
230	-13.422	-13.321	-13.234	-13.160	-13.095	-13.038	-12.989	-12.945	-12.907	-12.873
240	-13.581	-13.472	-13.379	-13.298	-13.228	-13.167	-13.113	-13.065	-13.023	-12.986
250	-13.733	-13.617	-13.518	-13.431	-13.356	-13.290	-13.232	-13.181	-13.135	-13.095
260	-13.881	-13.758	-13.652	-13.560	-13.480	-13.409	-13.347	-13.292	-13.243	-13.199
270	-14.024	-13.894	-13.782	-13.684	-13.599	-13.524	-13.458	-13.399	-13.347	-13.300
280	-14.164	-14.026	-13.908	-13.805	-13.715	-13.636	-13.566	-13.504	-13.448	-13.398
290	-14.300	-14.155	-14.030	-13.922	-13.828	-13.744	-13.670	-13.605	-13.546	-13.493
300	-14.434	-14.281	-14.150	-14.037	-13.937	-13.850	-13.772	-13.703	-13.641	-13.585
310	-14.565	-14.405	-14.268	-14.149	-14.044	-13.953	-13.871	-13.799	-13.734	-13.675
320	-14.694	-14.527	-14.383	-14.258	-14.149	-14.053	-13.968	-13.892	-13.824	-13.763
330	-14.821	-14.646	-14.496	-14.366	-14.252	-14.152	-14.063	-13.984	-13.913	-13.849
340	-14.947	-14.764	-14.607	-14.472	-14.353	-14.249	-14.156	-14.073	-13.999	-13.932
350	-15.070	-14.880	-14.717	-14.576	-14.452	-14.344	-14.247	-14.161	-14.084	-14.015
360	-15.192	-14.995	-14.826	-14.679	-14.550	-14.437	-14.337	-14.248	-14.168	-14.095
370	-15.313	-15.109	-14.933	-14.780	-14.647	-14.530	-14.426	-14.333	-14.250	-14.175
380	-15.431	-15.221	-15.038	-14.880	-14.742	-14.620	-14.513	-14.417	-14.330	-14.252
390	-15.548	-15.331	-15.143	-14.979	-14.836	-14.710	-14.599	-14.499	-14.410	-14.329
400	-15.662	-15.440	-15.246	-15.077	-14.929	-14.799	-14.684	-14.581	-14.488	-14.405

TABLE B-5. (continued)

ALTITUDE (km)	EXOSPHERIC TEMPERATURE (°K)									
	600	650	700	750	800	850	900	950	1000	1050
420	-15.884	-15.654	-15.449	-15.270	-15.112	-14.974	-14.851	-14.741	-14.642	-14.553
440	-16.094	-15.860	-15.647	-15.458	-15.292	-15.145	-15.014	-14.897	-14.793	-14.698
460	-16.290	-16.057	-15.839	-15.642	-15.467	-15.312	-15.174	-15.051	-14.940	-14.840
480	-16.468	-16.244	-16.024	-15.821	-15.639	-15.477	-15.332	-15.202	-15.085	-14.980
500	-16.627	-16.418	-16.200	-15.994	-15.806	-15.637	-15.486	-15.350	-15.227	-15.116
520	-16.765	-16.578	-16.367	-16.160	-15.969	-15.794	-15.637	-15.495	-15.367	-15.251
540	-16.882	-16.721	-16.522	-16.319	-16.125	-15.947	-15.785	-15.637	-15.504	-15.383
560	-16.982	-16.848	-16.664	-16.468	-16.275	-16.095	-15.929	-15.777	-15.639	-15.513
580	-17.065	-16.958	-16.793	-16.607	-16.418	-16.237	-16.068	-15.913	-15.770	-15.640
600	-17.137	-17.054	-16.908	-16.734	-16.552	-16.373	-16.203	-16.045	-15.899	-15.765
620	-17.199	-17.137	-17.010	-16.850	-16.677	-16.502	-16.333	-16.174	-16.025	-15.888
640	-17.255	-17.210	-17.100	-16.955	-16.792	-16.624	-16.457	-16.297	-16.147	-16.007
660	-17.305	-17.274	-17.179	-17.049	-16.898	-16.737	-16.575	-16.416	-16.265	-16.124
680	-17.351	-17.332	-17.250	-17.132	-16.993	-16.841	-16.685	-16.529	-16.379	-16.237
700	-17.394	-17.386	-17.314	-17.207	-17.079	-16.937	-16.788	-16.637	-16.488	-16.346
720	-17.434	-17.435	-17.371	-17.274	-17.156	-17.024	-16.883	-16.737	-16.592	-16.451
740	-17.473	-17.482	-17.425	-17.335	-17.227	-17.104	-16.971	-16.832	-16.691	-16.551
760	-17.510	-17.526	-17.475	-17.392	-17.290	-17.176	-17.051	-16.919	-16.783	-16.647
780	-17.545	-17.569	-17.523	-17.444	-17.348	-17.241	-17.125	-17.000	-16.870	-16.738
800	-17.579	-17.610	-17.568	-17.493	-17.402	-17.302	-17.192	-17.074	-16.950	-16.823
820	-17.612	-17.650	-17.612	-17.540	-17.452	-17.357	-17.253	-17.143	-17.025	-16.903
840	-17.644	-17.688	-17.654	-17.584	-17.500	-17.408	-17.310	-17.205	-17.094	-16.978
860	-17.674	-17.725	-17.695	-17.627	-17.545	-17.456	-17.363	-17.263	-17.158	-17.047
880	-17.703	-17.761	-17.735	-17.669	-17.588	-17.501	-17.411	-17.317	-17.217	-17.112
900	-17.732	-17.797	-17.774	-17.710	-17.630	-17.545	-17.457	-17.367	-17.272	-17.171
920	-17.759	-17.831	-17.812	-17.749	-17.670	-17.586	-17.501	-17.413	-17.322	-17.227
940	-17.785	-17.864	-17.850	-17.788	-17.709	-17.626	-17.542	-17.457	-17.370	-17.279
960	-17.811	-17.896	-17.886	-17.827	-17.748	-17.665	-17.582	-17.498	-17.414	-17.327
980	-17.835	-17.928	-17.922	-17.864	-17.786	-17.703	-17.620	-17.538	-17.456	-17.372
1000	-17.859	-17.958	-17.957	-17.901	-17.823	-17.739	-17.657	-17.576	-17.496	-17.414
1050	-17.915	-18.030	-18.042	-17.991	-17.913	-17.829	-17.746	-17.665	-17.587	-17.511
1100	-17.966	-18.097	-18.122	-18.078	-18.001	-17.915	-17.830	-17.749	-17.672	-17.597
1150	-18.014	-18.159	-18.198	-18.161	-18.086	-17.999	-17.912	-17.829	-17.751	-17.677
1200	-18.058	-18.217	-18.270	-18.241	-18.169	-18.081	-17.992	-17.907	-17.826	-17.751
1250	-18.100	-18.270	-18.337	-18.317	-18.249	-18.161	-18.070	-17.982	-17.900	-17.823
1300	-18.139	-18.319	-18.400	-18.391	-18.326	-18.239	-18.146	-18.056	-17.971	-17.893
1350	-18.176	-18.365	-18.458	-18.460	-18.401	-18.315	-18.221	-18.128	-18.041	-17.960
1400	-18.211	-18.408	-18.513	-18.526	-18.474	-18.389	-18.294	-18.199	-18.109	-18.026
1450	-18.245	-18.448	-18.564	-18.589	-18.544	-18.461	-18.365	-18.269	-18.177	-18.091
1500	-18.278	-18.485	-18.612	-18.649	-18.611	-18.532	-18.436	-18.337	-18.243	-18.155
1600	-18.340	-18.554	-18.699	-18.758	-18.738	-18.666	-18.571	-18.471	-18.372	-18.279
1700	-18.398	-18.617	-18.775	-18.855	-18.853	-18.793	-18.701	-18.599	-18.497	-18.400
1800	-18.454	-18.675	-18.843	-18.940	-18.958	-18.910	-18.824	-18.722	-18.618	-18.517
1900	-18.508	-18.729	-18.904	-19.017	-19.053	-19.020	-18.941	-18.841	-18.735	-18.630
2000	-18.560	-18.781	-18.960	-19.085	-19.138	-19.121	-19.051	-18.954	-18.847	-18.740
2100	-18.610	-18.829	-19.012	-19.146	-19.215	-19.213	-19.154	-19.062	-18.956	-18.847
2200	-18.659	-18.876	-19.060	-19.201	-19.283	-19.297	-19.251	-19.165	-19.060	-18.950
2300	-18.706	-18.921	-19.106	-19.252	-19.345	-19.374	-19.340	-19.262	-19.160	-19.050
2400	-18.752	-18.965	-19.149	-19.299	-19.402	-19.444	-19.423	-19.354	-19.256	-19.146
2500	-18.797	-19.007	-19.191	-19.343	-19.453	-19.507	-19.500	-19.440	-19.347	-19.239

TABLE B-5. (continued)

ALTITUDE (km)	EXOSPHERIC TEMPERATURE (°K)									
	1100	1150	1200	1250	1300	1350	1400	1450	1500	1550
90	-8.461	-8.461	-8.461	-8.461	-8.461	-8.461	-8.461	-8.461	-8.461	-8.461
92	-8.620	-8.620	-8.620	-8.620	-8.620	-8.620	-8.620	-8.620	-8.620	-8.620
94	-8.780	-8.780	-8.780	-8.780	-8.780	-8.780	-8.780	-8.781	-8.781	-8.781
96	-8.941	-8.942	-8.942	-8.942	-8.942	-8.942	-8.942	-8.942	-8.942	-8.942
98	-9.103	-9.103	-9.103	-9.103	-9.103	-9.104	-9.104	-9.104	-9.104	-9.104
100	-9.263	-9.263	-9.264	-9.264	-9.264	-9.264	-9.264	-9.265	-9.265	-9.265
102	-9.421	-9.422	-9.422	-9.422	-9.423	-9.423	-9.423	-9.423	-9.424	-9.424
104	-9.577	-9.577	-9.577	-9.578	-9.578	-9.578	-9.579	-9.579	-9.579	-9.579
106	-9.728	-9.728	-9.729	-9.729	-9.729	-9.730	-9.730	-9.730	-9.730	-9.730
108	-9.874	-9.875	-9.875	-9.875	-9.875	-9.876	-9.876	-9.876	-9.876	-9.876
110	-10.015	-10.015	-10.015	-10.015	-10.015	-10.016	-10.016	-10.016	-10.016	-10.016
115	-10.339	-10.338	-10.338	-10.337	-10.337	-10.336	-10.336	-10.336	-10.336	-10.335
120	-10.621	-10.619	-10.618	-10.617	-10.615	-10.614	-10.613	-10.613	-10.612	-10.611
125	-10.862	-10.860	-10.857	-10.855	-10.853	-10.851	-10.850	-10.848	-10.847	-10.846
130	-11.068	-11.064	-11.061	-11.058	-11.055	-11.052	-11.050	-11.048	-11.046	-11.044
135	-11.244	-11.239	-11.235	-11.231	-11.228	-11.225	-11.222	-11.219	-11.216	-11.214
140	-11.397	-11.391	-11.386	-11.382	-11.378	-11.374	-11.371	-11.368	-11.365	-11.362
145	-11.531	-11.525	-11.519	-11.515	-11.510	-11.506	-11.502	-11.499	-11.495	-11.492
150	-11.651	-11.644	-11.638	-11.633	-11.628	-11.623	-11.619	-11.615	-11.612	-11.609
155	-11.760	-11.752	-11.746	-11.740	-11.734	-11.729	-11.725	-11.721	-11.717	-11.714
160	-11.860	-11.851	-11.844	-11.837	-11.831	-11.826	-11.821	-11.817	-11.813	-11.809
170	-12.039	-12.029	-12.020	-12.012	-12.005	-11.998	-11.993	-11.988	-11.983	-11.979
180	-12.199	-12.186	-12.175	-12.166	-12.157	-12.149	-12.143	-12.137	-12.131	-12.126
190	-12.345	-12.330	-12.317	-12.305	-12.295	-12.286	-12.277	-12.270	-12.264	-12.258
200	-12.481	-12.463	-12.447	-12.433	-12.421	-12.410	-12.401	-12.392	-12.384	-12.377
210	-12.608	-12.587	-12.569	-12.553	-12.539	-12.526	-12.515	-12.505	-12.495	-12.487
220	-12.729	-12.705	-12.684	-12.666	-12.649	-12.635	-12.621	-12.610	-12.599	-12.590
230	-12.844	-12.817	-12.794	-12.773	-12.754	-12.737	-12.722	-12.709	-12.697	-12.686
240	-12.953	-12.924	-12.898	-12.875	-12.854	-12.835	-12.818	-12.803	-12.789	-12.776
250	-13.059	-13.027	-12.998	-12.972	-12.949	-12.928	-12.909	-12.892	-12.877	-12.863
260	-13.160	-13.126	-13.094	-13.066	-13.041	-13.018	-12.997	-12.978	-12.961	-12.945
270	-13.259	-13.221	-13.187	-13.157	-13.129	-13.104	-13.081	-13.060	-13.042	-13.024
280	-13.353	-13.313	-13.277	-13.244	-13.214	-13.187	-13.163	-13.140	-13.120	-13.101
290	-13.446	-13.403	-13.364	-13.329	-13.297	-13.268	-13.242	-13.217	-13.195	-13.175
300	-13.535	-13.490	-13.449	-13.411	-13.377	-13.346	-13.318	-13.292	-13.268	-13.246
310	-13.622	-13.575	-13.531	-13.492	-13.456	-13.423	-13.393	-13.365	-13.340	-13.316
320	-13.707	-13.657	-13.612	-13.570	-13.532	-13.497	-13.465	-13.436	-13.409	-13.384
330	-13.791	-13.738	-13.690	-13.647	-13.607	-13.570	-13.536	-13.505	-13.477	-13.450
340	-13.872	-13.817	-13.767	-13.721	-13.679	-13.641	-13.606	-13.573	-13.543	-13.515
350	-13.952	-13.894	-13.842	-13.794	-13.751	-13.711	-13.673	-13.639	-13.608	-13.578
360	-14.030	-13.970	-13.916	-13.866	-13.821	-13.779	-13.740	-13.704	-13.671	-13.640
370	-14.107	-14.045	-13.988	-13.937	-13.889	-13.846	-13.805	-13.768	-13.733	-13.701
380	-14.182	-14.118	-14.059	-14.006	-13.957	-13.911	-13.869	-13.831	-13.795	-13.761
390	-14.256	-14.190	-14.129	-14.074	-14.023	-13.976	-13.932	-13.892	-13.855	-13.820
400	-14.330	-14.261	-14.198	-14.141	-14.088	-14.039	-13.994	-13.952	-13.914	-13.878

TABLE B-5. (continued)

ALTITUDE (km)	EXOSPHERIC TEMPERATURE (°K)									
	1100	1150	1200	1250	1300	1350	1400	1450	1500	1550
420	-14.473	-14.400	-14.333	-14.272	-14.215	-14.163	-14.115	-14.071	-14.029	-13.990
440	-14.613	-14.535	-14.464	-14.399	-14.339	-14.284	-14.233	-14.185	-14.141	-14.100
460	-14.750	-14.668	-14.592	-14.524	-14.460	-14.402	-14.347	-14.297	-14.250	-14.207
480	-14.884	-14.797	-14.718	-14.645	-14.578	-14.517	-14.459	-14.406	-14.357	-14.311
500	-15.016	-14.925	-14.841	-14.765	-14.694	-14.629	-14.569	-14.513	-14.461	-14.412
520	-15.146	-15.050	-14.962	-14.882	-14.808	-14.739	-14.676	-14.617	-14.563	-14.512
540	-15.273	-15.173	-15.081	-14.997	-14.919	-14.848	-14.782	-14.720	-14.663	-14.609
560	-15.398	-15.294	-15.198	-15.110	-15.029	-14.954	-14.885	-14.821	-14.761	-14.705
580	-15.521	-15.413	-15.313	-15.222	-15.137	-15.059	-14.987	-14.920	-14.858	-14.799
600	-15.643	-15.530	-15.427	-15.331	-15.244	-15.163	-15.088	-15.018	-14.953	-14.892
620	-15.761	-15.645	-15.538	-15.440	-15.349	-15.265	-15.187	-15.114	-15.046	-14.983
640	-15.878	-15.758	-15.648	-15.546	-15.452	-15.365	-15.284	-15.209	-15.139	-15.073
660	-15.992	-15.869	-15.756	-15.651	-15.554	-15.464	-15.380	-15.302	-15.230	-15.162
680	-16.103	-15.978	-15.862	-15.754	-15.654	-15.561	-15.475	-15.395	-15.320	-15.250
700	-16.211	-16.084	-15.966	-15.856	-15.753	-15.658	-15.569	-15.486	-15.408	-15.336
720	-16.316	-16.188	-16.067	-15.955	-15.850	-15.752	-15.661	-15.576	-15.496	-15.421
740	-16.417	-16.288	-16.166	-16.052	-15.945	-15.845	-15.752	-15.664	-15.582	-15.506
760	-16.514	-16.385	-16.263	-16.147	-16.039	-15.937	-15.841	-15.751	-15.667	-15.589
780	-16.607	-16.479	-16.357	-16.240	-16.130	-16.026	-15.929	-15.837	-15.751	-15.670
800	-16.695	-16.569	-16.447	-16.330	-16.219	-16.114	-16.015	-15.922	-15.834	-15.751
820	-16.779	-16.655	-16.534	-16.418	-16.306	-16.200	-16.099	-16.005	-15.915	-15.831
840	-16.858	-16.737	-16.618	-16.502	-16.391	-16.284	-16.182	-16.086	-15.995	-15.909
860	-16.932	-16.815	-16.698	-16.584	-16.472	-16.365	-16.263	-16.166	-16.074	-15.986
880	-17.002	-16.889	-16.775	-16.662	-16.552	-16.445	-16.342	-16.244	-16.151	-16.062
900	-17.066	-16.958	-16.847	-16.737	-16.628	-16.521	-16.419	-16.320	-16.226	-16.137
920	-17.127	-17.023	-16.916	-16.808	-16.701	-16.596	-16.493	-16.395	-16.300	-16.210
940	-17.183	-17.084	-16.981	-16.876	-16.771	-16.667	-16.566	-16.467	-16.372	-16.281
960	-17.236	-17.140	-17.042	-16.940	-16.838	-16.736	-16.635	-16.537	-16.442	-16.351
980	-17.285	-17.194	-17.099	-17.001	-16.902	-16.802	-16.703	-16.605	-16.511	-16.419
1000	-17.331	-17.243	-17.152	-17.058	-16.962	-16.865	-16.767	-16.671	-16.577	-16.485
1050	-17.434	-17.354	-17.273	-17.187	-17.099	-17.009	-16.917	-16.825	-16.733	-16.643
1100	-17.524	-17.450	-17.375	-17.298	-17.218	-17.135	-17.050	-16.963	-16.876	-16.789
1150	-17.605	-17.535	-17.465	-17.394	-17.321	-17.245	-17.167	-17.086	-17.004	-16.921
1200	-17.680	-17.612	-17.545	-17.478	-17.410	-17.341	-17.269	-17.195	-17.118	-17.041
1250	-17.751	-17.683	-17.618	-17.554	-17.490	-17.425	-17.359	-17.290	-17.220	-17.147
1300	-17.819	-17.751	-17.686	-17.623	-17.562	-17.500	-17.438	-17.374	-17.309	-17.242
1350	-17.885	-17.815	-17.750	-17.688	-17.627	-17.568	-17.509	-17.449	-17.388	-17.326
1400	-17.949	-17.878	-17.811	-17.749	-17.689	-17.631	-17.574	-17.517	-17.460	-17.401
1450	-18.012	-17.939	-17.871	-17.807	-17.747	-17.690	-17.634	-17.579	-17.524	-17.469
1500	-18.073	-17.998	-17.929	-17.864	-17.803	-17.745	-17.690	-17.636	-17.583	-17.530
1600	-18.193	-18.114	-18.040	-17.973	-17.910	-17.850	-17.795	-17.741	-17.690	-17.640
1700	-18.309	-18.226	-18.148	-18.077	-18.011	-17.950	-17.892	-17.838	-17.786	-17.737
1800	-18.422	-18.334	-18.253	-18.178	-18.109	-18.044	-17.985	-17.929	-17.876	-17.826
1900	-18.532	-18.440	-18.355	-18.276	-18.204	-18.136	-18.074	-18.015	-17.961	-17.909
2000	-18.638	-18.543	-18.454	-18.372	-18.296	-18.225	-18.160	-18.099	-18.042	-17.989
2100	-18.742	-18.643	-18.550	-18.465	-18.386	-18.312	-18.244	-18.181	-18.121	-18.066
2200	-18.842	-18.740	-18.645	-18.556	-18.473	-18.397	-18.326	-18.260	-18.198	-18.141
2300	-18.940	-18.835	-18.736	-18.644	-18.558	-18.479	-18.405	-18.337	-18.273	-18.213
2400	-19.035	-18.927	-18.825	-18.730	-18.642	-18.559	-18.483	-18.412	-18.346	-18.284
2500	-19.126	-19.017	-18.912	-18.814	-18.723	-18.638	-18.559	-18.485	-18.417	-18.353

TABLE B-5. (continued)

ALTITUDE (km)	EXOSPHERIC TEMPERATURE (°K)								
	1600	1650	1700	1750	1800	1850	1900	1950	2000
90	-8.461	-8.461	-8.461	-8.461	-8.461	-8.461	-8.461	-8.461	-8.461
92	-8.620	-8.620	-8.620	-8.620	-8.620	-8.620	-8.620	-8.620	-8.620
94	-8.781	-8.781	-8.781	-8.781	-8.781	-8.781	-8.781	-8.781	-8.781
96	-8.942	-8.942	-8.942	-8.942	-8.943	-8.943	-8.943	-8.943	-8.943
98	-9.104	-9.104	-9.104	-9.104	-9.105	-9.105	-9.105	-9.105	-9.105
100	-9.265	-9.265	-9.265	-9.265	-9.266	-9.266	-9.266	-9.266	-9.266
102	-9.424	-9.424	-9.424	-9.424	-9.425	-9.425	-9.425	-9.425	-9.425
104	-9.580	-9.580	-9.580	-9.580	-9.580	-9.580	-9.580	-9.581	-9.581
106	-9.731	-9.731	-9.731	-9.731	-9.731	-9.731	-9.732	-9.732	-9.732
108	-9.876	-9.876	-9.877	-9.877	-9.877	-9.877	-9.877	-9.877	-9.877
110	-10.016	-10.016	-10.016	-10.016	-10.016	-10.016	-10.016	-10.016	-10.016
115	-10.335	-10.335	-10.335	-10.334	-10.334	-10.334	-10.334	-10.334	-10.333
120	-10.610	-10.610	-10.609	-10.608	-10.608	-10.607	-10.607	-10.606	-10.606
125	-10.844	-10.843	-10.842	-10.841	-10.840	-10.839	-10.838	-10.838	-10.837
130	-11.042	-11.041	-11.039	-11.038	-11.036	-11.035	-11.034	-11.033	-11.032
135	-11.212	-11.210	-11.208	-11.206	-11.205	-11.203	-11.201	-11.200	-11.199
140	-11.359	-11.357	-11.355	-11.353	-11.351	-11.349	-11.347	-11.346	-11.344
145	-11.490	-11.487	-11.485	-11.482	-11.480	-11.478	-11.476	-11.474	-11.472
150	-11.606	-11.603	-11.600	-11.598	-11.596	-11.593	-11.591	-11.589	-11.587
155	-11.711	-11.708	-11.705	-11.702	-11.700	-11.697	-11.695	-11.693	-11.691
160	-11.806	-11.803	-11.800	-11.797	-11.795	-11.792	-11.790	-11.788	-11.786
170	-11.975	-11.972	-11.968	-11.965	-11.962	-11.960	-11.957	-11.955	-11.953
180	-12.122	-12.118	-12.114	-12.111	-12.108	-12.105	-12.102	-12.099	-12.097
190	-12.253	-12.248	-12.244	-12.240	-12.236	-12.233	-12.230	-12.227	-12.224
200	-12.371	-12.366	-12.361	-12.356	-12.352	-12.348	-12.344	-12.341	-12.338
210	-12.480	-12.473	-12.467	-12.462	-12.457	-12.452	-12.448	-12.444	-12.441
220	-12.581	-12.573	-12.566	-12.560	-12.554	-12.549	-12.544	-12.539	-12.535
230	-12.676	-12.667	-12.659	-12.651	-12.644	-12.638	-12.632	-12.627	-12.622
240	-12.765	-12.755	-12.745	-12.737	-12.729	-12.722	-12.715	-12.709	-12.704
250	-12.850	-12.838	-12.828	-12.818	-12.809	-12.801	-12.793	-12.786	-12.780
260	-12.931	-12.918	-12.906	-12.895	-12.885	-12.876	-12.867	-12.859	-12.852
270	-13.009	-12.994	-12.981	-12.969	-12.958	-12.947	-12.938	-12.929	-12.920
280	-13.084	-13.068	-13.053	-13.040	-13.027	-13.016	-13.005	-12.995	-12.986
290	-13.156	-13.139	-13.123	-13.108	-13.094	-13.082	-13.070	-13.059	-13.049
300	-13.226	-13.208	-13.190	-13.174	-13.160	-13.146	-13.133	-13.121	-13.110
310	-13.294	-13.274	-13.256	-13.239	-13.223	-13.208	-13.194	-13.181	-13.169
320	-13.361	-13.340	-13.320	-13.301	-13.284	-13.268	-13.253	-13.239	-13.226
330	-13.426	-13.403	-13.382	-13.362	-13.344	-13.327	-13.311	-13.296	-13.282
340	-13.489	-13.465	-13.443	-13.422	-13.402	-13.384	-13.367	-13.351	-13.336
350	-13.551	-13.526	-13.502	-13.480	-13.460	-13.440	-13.422	-13.405	-13.389
360	-13.612	-13.585	-13.560	-13.537	-13.516	-13.495	-13.476	-13.458	-13.441
370	-13.671	-13.644	-13.618	-13.593	-13.571	-13.549	-13.529	-13.510	-13.492
380	-13.730	-13.701	-13.674	-13.648	-13.624	-13.602	-13.581	-13.561	-13.542
390	-13.787	-13.757	-13.729	-13.702	-13.677	-13.654	-13.632	-13.611	-13.592
400	-13.844	-13.813	-13.783	-13.755	-13.730	-13.705	-13.682	-13.660	-13.640

TABLE B-5. (concluded)

ALTITUDE (km)	EXOSPHERIC TEMPERATURE (°K)								
	1600	1650	1700	1750	1800	1850	1900	1950	2000
420	-13.954	-13.921	-13.889	-13.859	-13.831	-13.805	-13.780	-13.757	-13.734
440	-14.062	-14.026	-13.992	-13.960	-13.930	-13.902	-13.875	-13.850	-13.826
460	-14.166	-14.128	-14.092	-14.058	-14.026	-13.996	-13.968	-13.941	-13.915
480	-14.268	-14.227	-14.189	-14.153	-14.120	-14.088	-14.058	-14.029	-14.002
500	-14.367	-14.324	-14.284	-14.247	-14.211	-14.177	-14.146	-14.116	-14.087
520	-14.464	-14.419	-14.377	-14.338	-14.300	-14.265	-14.232	-14.200	-14.170
540	-14.559	-14.513	-14.468	-14.427	-14.388	-14.351	-14.316	-14.283	-14.251
560	-14.653	-14.604	-14.558	-14.515	-14.474	-14.435	-14.398	-14.364	-14.331
580	-14.745	-14.694	-14.646	-14.600	-14.558	-14.517	-14.479	-14.443	-14.409
600	-14.835	-14.782	-14.732	-14.685	-14.640	-14.598	-14.559	-14.521	-14.485
620	-14.924	-14.869	-14.817	-14.768	-14.722	-14.678	-14.637	-14.598	-14.560
640	-15.012	-14.955	-14.901	-14.850	-14.802	-14.757	-14.714	-14.673	-14.634
660	-15.099	-15.039	-14.983	-14.931	-14.881	-14.834	-14.789	-14.747	-14.707
680	-15.184	-15.122	-15.065	-15.010	-14.959	-14.910	-14.864	-14.820	-14.779
700	-15.268	-15.205	-15.145	-15.089	-15.035	-14.985	-14.937	-14.892	-14.849
720	-15.351	-15.286	-15.224	-15.166	-15.111	-15.059	-15.010	-14.964	-14.919
740	-15.434	-15.366	-15.302	-15.242	-15.186	-15.132	-15.082	-15.034	-14.988
760	-15.515	-15.445	-15.380	-15.318	-15.260	-15.205	-15.153	-15.103	-15.056
780	-15.595	-15.523	-15.456	-15.393	-15.333	-15.276	-15.223	-15.172	-15.123
800	-15.674	-15.600	-15.531	-15.466	-15.405	-15.347	-15.292	-15.239	-15.190
820	-15.751	-15.677	-15.606	-15.539	-15.476	-15.416	-15.360	-15.306	-15.255
840	-15.828	-15.752	-15.679	-15.611	-15.547	-15.485	-15.427	-15.372	-15.320
860	-15.904	-15.826	-15.752	-15.682	-15.616	-15.554	-15.494	-15.438	-15.384
880	-15.978	-15.899	-15.824	-15.752	-15.685	-15.621	-15.560	-15.502	-15.447
900	-16.051	-15.971	-15.894	-15.822	-15.753	-15.687	-15.625	-15.566	-15.510
920	-16.123	-16.042	-15.964	-15.890	-15.820	-15.753	-15.690	-15.629	-15.572
940	-16.194	-16.111	-16.032	-15.957	-15.886	-15.818	-15.753	-15.692	-15.633
960	-16.263	-16.179	-16.100	-16.023	-15.951	-15.882	-15.816	-15.754	-15.694
980	-16.331	-16.247	-16.166	-16.089	-16.015	-15.945	-15.878	-15.815	-15.754
1000	-16.397	-16.312	-16.231	-16.153	-16.078	-16.007	-15.940	-15.875	-15.813
1050	-16.556	-16.470	-16.388	-16.308	-16.232	-16.159	-16.089	-16.022	-15.958
1100	-16.703	-16.619	-16.536	-16.456	-16.379	-16.304	-16.233	-16.164	-16.098
1150	-16.839	-16.756	-16.675	-16.596	-16.518	-16.443	-16.371	-16.300	-16.233
1200	-16.962	-16.883	-16.804	-16.726	-16.650	-16.575	-16.502	-16.431	-16.362
1250	-17.073	-16.998	-16.923	-16.847	-16.772	-16.699	-16.626	-16.555	-16.486
1300	-17.173	-17.102	-17.031	-16.958	-16.886	-16.814	-16.743	-16.673	-16.604
1350	-17.262	-17.196	-17.128	-17.060	-16.991	-16.921	-16.852	-16.783	-16.715
1400	-17.341	-17.279	-17.216	-17.152	-17.086	-17.020	-16.953	-16.886	-16.820
1450	-17.412	-17.355	-17.295	-17.235	-17.173	-17.110	-17.046	-16.981	-16.917
1500	-17.477	-17.422	-17.367	-17.310	-17.251	-17.192	-17.131	-17.069	-17.007
1600	-17.590	-17.540	-17.490	-17.439	-17.387	-17.334	-17.280	-17.224	-17.168
1700	-17.689	-17.641	-17.595	-17.548	-17.501	-17.453	-17.404	-17.354	-17.303
1800	-17.778	-17.731	-17.686	-17.642	-17.597	-17.553	-17.508	-17.463	-17.417
1900	-17.860	-17.814	-17.769	-17.725	-17.683	-17.641	-17.598	-17.556	-17.514
2000	-17.939	-17.891	-17.846	-17.802	-17.760	-17.719	-17.678	-17.638	-17.598
2100	-18.014	-17.965	-17.919	-17.874	-17.832	-17.791	-17.751	-17.712	-17.673
2200	-18.087	-18.036	-17.988	-17.943	-17.900	-17.859	-17.819	-17.780	-17.742
2300	-18.157	-18.105	-18.056	-18.009	-17.965	-17.923	-17.882	-17.843	-17.805
2400	-18.226	-18.172	-18.121	-18.073	-18.027	-17.984	-17.943	-17.903	-17.865
2500	-18.293	-18.237	-18.184	-18.135	-18.088	-18.043	-18.001	-17.961	-17.922

APPENDIX C
GLOSSARY*

Atmospheric Density – Same as **Mass Density**.

Celestial Longitude – The arc of the ecliptic between the vernal equinox and the point at which the celestial longitude is given. It is always measured eastward from the vernal equinox, completely around the ecliptic, from 0° to 360°.

Daily 10.7 cm Flux – Assumed to be the same as radio flux. A measured indicator for the amount of EUV solar radiation received by the Earth. See **Radio Flux**.

Declination – In the geocentric coordinate system, it is the angular distance along the meridian of a point of a body from the equator. Declination is analogous to latitude on Earth. It is taken positive north of the equator and negative south of the equator.

Density – See **Mass Density** and **Number Density**.

Density Bulge – A slight bulge in the daylight portion of the atmosphere that is caused by atmospheric heating. The center of the bulge follows the Sun, lagging by two hours, and also migrates north and south with the sub-solar point. A slight depression in the dark portion of the atmosphere (anti-bulge), which is a product of the bulge, is centered eleven hours earlier at 0300 local time. At any given height above 120 km, the maximum density occurs at the center of the density bulge.

Density Scale Height – The scale height of a point in the atmosphere is a numerical quantity that represents the altitude above the point at which the mass density would decrease by a factor of 1/e (the exponential log e) from the density at the point. See equation A-35.

Diffusive Equilibrium – The steady state resulting from the diffusive process in which the constituent gases of the atmosphere are distributed independently of one another. In such a state, the number density of the heavier constituents decreases more rapidly with altitude than that of the lighter constituents.

Diurnal Effect – The day-to-night variation in nearly all atmospheric parameters that is caused by the rotation of the Earth. See **Density Bulge**.

Ecliptic – The apparent path of the Sun about the Earth during a year. Strictly, it is the projection of the plane of the Earth's orbit on the celestial sphere.

Electromagnetic Radiation – Energy that is propagated through space, primarily from the Sun, in the form of an advancing disturbance in electric and magnetic fields (often called radiation).

Exosphere – The outermost, or topmost, portion of the atmosphere. Its lower boundary is the critical level of escape, variously estimated at 350 to 750 km above the Earth's surface.

*Cross references within the glossary are indicated by bold face.

Exospheric Temperature – The value that the atmospheric temperature reaches near 350 km altitude. Above this altitude, temperature is considered to be isothermal (lapse rate of zero) and to range from 650° to 2100°K

Geomagnetic Index – A measurement of the most active component of the magnetic field made by surface magnetic observatories (an average of 12 selected stations) at three-hour intervals. The measurement is made in the units of gauss or gamma (1 gauss = 10^5 gammas), but observations are reported in terms of a unitless quantity (a_p) which varies from 0 to 400.

Gravity Wave – A wave disturbance in which buoyancy acts as the restoring force on parcels displaced from hydrostatic equilibrium.

Heat Conductivity – An intrinsic physical property of a substance, describing its ability to conduct heat as a consequence of molecular motion.

Heterosphere – The upper portion of the two-part division of the atmosphere according to the general homogeniety of atmospheric composition; the layer above the homosphere. The heterosphere is characterized by variation in composition, and mean molecular weight of constituent gases. The region starts at 80 to 100 km above the Earth, and therefore closely coincides with the ionosphere and the thermosphere.

Homosphere – The lower portion of a two-part division of the atmosphere according to the general homogeniety of atmospheric composition; opposed to the heterosphere. The homosphere is the region in which there is no gross change in atmospheric composition, that is, all of the atmosphere from the Earth's surface to about 80 to 100 km.

Homopause – The top of the homosphere, or the level of transition between it and the heterosphere. It probably lies between 80 and 90 km, where molecular oxygen begins to dissociate into atomic oxygen. The homopause is somewhat lower in the daytime than at night.

Hour Angle – The angular distance measured eastward or westward along the celestial equator to the longitude of the point for which the hour angle refers. Morning hour angles are negative and afternoon are positive.

Hydrostatic Equilibrium – The state of a fluid whose surfaces of constant pressure and constant mass (or density) coincide and are horizontal throughout; a complete balance exists between the force of gravity and the pressure force.

Ionization – In atmospheric electricity, the process by which neutral atmospheric molecules or other suspended particles are rendered electrically charged chiefly by collisions with high-energy particles. Cosmic rays and emanations from radioactive gasses are the main sources of atmospheric ionization. In the lower atmosphere, decay electrons of mu-mesons plus alpha particles from radioactive gases, as well as beta particles and gamma rays, serve to ionize air molecules.

Julian Date (also Julian day) – Number of days measured from January 1 (noon GMT), 4713 B.C.

Lapse Rate – The change in temperature with increasing altitude.

Magnetic Field – A region wherein any magnetic dipole would experience a magnetic force or torque.

Mass Density – The ratio of the mass of any substance to the volume occupied by it (usually expressed in gm/cm^3).

Mean Free Path – The average distance traveled by the molecules of a perfect gas between consecutive collisions with one another.

Mesosphere – The atmospheric shell between about 20 km and about 70 or 80 km, extending from the top of the stratosphere to the upper temperature minimum (the mesopause). It is characterized by a broad temperature maximum (the mesopeak) at about 50 km, except possibly over the winter polar regions.

Mixing – A random exchange of atmospheric constituents caused primarily by non-homogeneous pressure forces.

Modified Julian Day – Number of days measured from November 17, 1858 (midnight GMT).

Number Density – The numerical count of molecules of a particular constituent for a given volume (usually given as $number/cm^3$).

Photodissociation – The dissociation (splitting) of a molecule by the absorption of a photon. The resulting components may be ionized in the process (photoionization).

Radio Flux (F10.7) – The radio flux density at 10.7 cm is a useful indicator of solar activity as it exhibits both 11-year and 27-day periodicities. Its high correlation with the solar radiation which is absorbed in the upper atmosphere makes it a desirable weighting function for representing the effects of this absorption in a model atmosphere. The standard data source is Ottawa, Canada, although it is measured at several observatories. The solar flux is actually measured over a complete bandwidth to increase the faithfulness of the radio energy input as it passes through the receiver and therefore must be divided by width of the band. The 10.7 cm solar flux has units of 10^{-22} watts/sq m/sec/bandwidth but should be considered as a unitless quantity for the equations herein.

Right Ascension – The angular distance measured from the vernal equinox eastward along the celestial equator to the longitude of the point to which the right ascension refers.

Solar Radiation – The total electromagnetic radiation and corpuscular radiation emitted by the Sun.

Solar Wind – The flux of plasma from the Sun.

Static Diffusion – Same as **Diffusive Equilibrium.**

Stratosphere – The atmospheric shell above the troposphere and below the mesosphere. It extends, therefore, from the tropopause to the height where the temperature begins to increase in the 20 to 25 km region.

Sunspot Number – A solar index which has been compiled back to 1600 A.D. The sunspot number takes into account the number of sunspot groups as well as the number of individual spots. It can be computed from the formula

$$R = K\,(10g + s)$$

where

R = sunspot number

g = number of groups

s = number of spots

K = a constant, roughly equal to 1

K is used to adjust individual R numbers to account for some observatories having better observing conditions than others.

Thermosphere – The region of the atmosphere extending upward from about 85 km to the exosphere. In this region the temperature increases with altitude to about 350 km and then is constant with increasing altitude.

Thermopause – The top of the thermosphere, or the level of transition between it and the exosphere.

81-Day Mean Solar Flux – The arithmetic average of the daily 10.7 cm solar flux values for the 81 days preceding the day for which the 81-day mean is given.

NASA SPACE VEHICLE DESIGN CRITERIA MONOGRAPHS

ENVIRONMENT

SP-8005	Solar Electromagnetic Radiation, revised May 1971
SP-8010	Models of Mars Atmosphere (1967), May 1968
SP-8011	Models of Venus Atmosphere (1972), revised September 1972
SP-8013	Meteoroid Environment Model–1969 (Near Earth to Lunar Surface), March 1969
SP-8017	Magnetic Fields–Earth and Extraterrestrial, March 1969
SP-8020	Mars Surface Models (1968), May 1969
SP-8021	Models of Earth's Atmosphere (190 to 2500 km), revised March 1973
SP-8023	Lunar Surface Models, May 1969
SP-8037	Assessment and Control of Spacecraft Magnetic Fields, September 1970
SP-8038	Meteoroid Environment Model–1970 (Interplanetary and Planetary), October 1970
SP-8049	The Earth's Ionosphere, March 1971
SP-8067	Earth Albedo and Emitted Radiation, July 1971
SP-8069	The Planet Jupiter (1970), December 1971
SP-8084	Surface Atmospheric Extremes (Launch and Transportation Areas), May 1972
SP-8085	The Planet Mercury (1971), March 1972
SP-8091	The Planet Saturn (1970), June 1972
SP-8092	Assessment and Control of Spacecraft Electromagnetic Interference, June 1972

SP-8103	The Planets Uranus, Nepture, and Pluto (1971), November 1972
SP-8105	Spacecraft Thermal Control, May 1973

STRUCTURES

SP-8001	Buffeting During Atmospheric Ascent, revised November 1970
SP-8002	Flight-Loads Measurements During Launch and Exit, revised June 1972
SP-8003	Flutter, Buzz, and Divergence, July 1964
SP-8004	Panel Flutter, revised June 1972
SP-8006	Local Steady Aerodynamic Loads During Launch and Exit, May 1965
SP-8007	Buckling of Thin-Walled Circular Cylinders, revised August 1968
SP-8008	Prelaunch Ground Wind Loads, November 1965
SP-8009	Propellant Slosh Loads, August 1968
SP-8012	Natural Vibration Modal Analysis, September 1968
SP-8014	Entry Thermal Protection, August 1968
SP-8019	Buckling of Thin-Walled Truncated Cones, September 1968
SP-8022	Staging Loads, February 1969
SP-8029	Aerodynamic and Rocket-Exhaust Heating During Launch and Ascent, May 1969
SP-8031	Slosh Suppression, May 1969
SP-8032	Buckling of Thin-Walled Doubly Curved Shells, August 1969
SP-8035	Wind Loads During Ascent, June 1970
SP-8040	Fracture Control of Metallic Pressure Vessels, May 1970
SP-8042	Meteoroid Damage Assessment, May 1970
SP-8043	Design–Development testing, May 1970

SP-8044	Qualification testing, May 1970
SP-8045	Acceptance testing, April 1970
SP-8046	Landing Impact Attenuation for Non-Surface-Planing Landers, April 1970
SP-8050	Structural Vibration Prediction, June 1970
SP-8053	Nuclear and Space Radiation Effects on Materials, June 1970
SP-8054	Space Radiation Protection, June 1970
SP-8055	Prevention of Coupled Structure-Propulsion Instability (Pogo), October 1970
SP-8056	Flight Separation Mechanisms, October 1970
SP-8057	Structural Design Criteria Applicable to a Space Shuttle, revised March 1972
SP-8060	Compartment Venting, November 1970
SP-8061	Interaction with Umblicals and Launch Stand, August 1970
SP-8062	Entry Gasdynamic Heating, January 1971
SP-8063	Lubrication, Friction, and Wear, June 1971
SP-8066	Deployable Aerodynamic Deceleration Systems, June 1971
SP-8068	Buckling Strength of Structural Plates, June 1971
SP-8072	Acoustic Loads Generated by the Propulsion System, June 1971
SP-8077	Transportation and Handling Loads, September 1971
SP-8079	Structural Interaction with Control Systems, November 1971
SP-8082	Stress-Corrosion Cracking in Metals, August 1971
SP-8083	Discontinuity in Metallic Pressure Vessels, November 1971
SP-8095	Preliminary Criteria for the Fracture Control of Space Shuttle Structures, June 1971

SP-8099	Combining Ascent Loads, May 1972

GUIDANCE AND CONTROL

SP-8015	Guidance and Navigation for Entry Vehicles, November 1968
SP-8016	Effects of Structural Flexibility on Spacecraft Control Systems, April 1969
SP-8018	Spacecraft Magnetic Torques, March 1969
SP-8024	Spacecraft Gravitational Torques, May 1969
SP-8026	Spacecraft Star Trackers, July 1970
SP-8027	Spacecraft Radiation Torques, October 1969
SP-8028	Entry Vehicle Control, November 1969
SP-8033	Spacecraft Earth Horizon Sensors, December 1969
SP-8034	Spacecraft Mass Expulsion Torques, December 1969
SP-8036	Effects of Structural Flexibility on Launch Vehicle Control Systems, February 1970
SP-8047	Spacecraft Sun Sensors, June 1970
SP-8058	Spacecraft Aerodynamic Torques, January 1971
SP-8059	Spacecraft Attitude Control During Thrusting Maneuvers, February 1971
SP-8065	Tubular Spacecraft Booms (Extendible, Reel Stored), February 1971
SP-8070	Spaceborne Digital Computer Systems, March 1971
SP-8071	Passive Gravity-Gradient Libration Dampers, February 1971
SP-8074	Spacecraft Solar Cell Arrays, May 1971
SP-8078	Spaceborne Electronic Imaging Systems, June 1971
SP-8086	Space Vehicle Displays Design Criteria, March 1972

SP-8096	Space Vehicle Gyroscope Sensor Applications, October 1972
SP-8098	Effects of Structural Flexibility on Entry Vehicle Control Systems, June 1972
SP-8102	Space Vehicle Accelerometer Applications, December 1972

CHEMICAL PROPULSION

SP-8025	Solid Rocket Motor Metal Cases, April 1970
SP-8039	Solid Rocket Motor Performance Analysis and Prediction, May 1971
SP-8041	Captive-Fired Testing of Solid Rocket Motors, March 1971
SP-8048	Liquid Rocket Engine Turbopump Bearings, March 1971
SP-8051	Solid Rocket Motor Igniters, March 1971
SP-8052	Liquid Rocket Engine Turbopump Inducers, May 1971
SP-8064	Solid Propellant Selection and Characterization, June 1971
SP-8075	Solid Propellant Processing Factors in Rocket Motor Design, October 1971
SP-8076	Solid Propellant Grain Design and Internal Ballistics, March 1972

NASA-Langley, 1973